

UNITED STATES DEPARTMENT OF THE INTERIOR
GEOLOGICAL SURVEY

An Evaluation of Electric Geophysical Techniques
for Ground Water Exploration in Truk,
Federated States of Micronesia

by

Jim Kauahikaua

Open-File Report 87-146

This report is preliminary and has not been reviewed for conformity with U.S. Geological Survey editorial standards and stratigraphic nomenclature. The use of trade names is solely for descriptive purposes and does not imply endorsement by the Geological Survey.

1987

ABSTRACT

In April, 1983, three electrical resistivity techniques were evaluated for ground water exploration in the Truk Islands. The techniques evaluated were Direct Current (DC) Schlumberger sounding, Max/Min electromagnetic (EM) profiling and Very Low Frequency (VLF) profiling. Some aquifer properties were successfully determined by the DC and EM techniques. The DC technique was especially useful in the volcanic islands whereas the EM technique was most useful in the coralline islands. Because of the large distance to VLF transmitters, the VLF technique was not useful in the study area.

INTRODUCTION

Truk is one of the Eastern Caroline Islands formerly part of the Trust Territory of the Pacific and now part of the Federated States of Micronesia. Geologically, it is unique in that it is in the middle of its evolution from a volcanic island (like Hawai'i) to an atoll. Truk has a ring of coralline islands that would normally make it a large atoll; however, it also has a handful of weathered volcanic peaks, that are remnants of the volcanic edifice upon which the coralline islands are built, subsiding into the center of its lagoon (Stark and Hay, 1963). The coralline islands are known as 'low islands' because of their generally low elevations. The weathered volcanic islands are known as 'high islands' because of their generally higher elevations.

Not surprisingly, the hydrology of high and low islands is very different. The high islands are primarily composed of poorly permeable volcanic lava flows. Weathering increases their permeability by a small but significant amount. The permeability is higher still in the alluvium making up the bases of slopes at and below sea level (Takasaki, written communication, 1983). The use of electric geophysical techniques might aid hydrologists in this environment by making some determinations about the nature and size of the aquifer (e.g., whether it is weathered volcanics or alluvium), and whether it contains fresh or brackish water.

The low islands are mostly composed of very permeable coralline rocks. Freshwater occurs in lenses which float on saline water. The boundary between fresh and saline water is marked by a zone of transitional salinities - the transition zone. The techniques of electrical geophysics could be used to map the thickness of the freshwater lens by first mapping the depth to the middle of the transition zone between fresh and saline water and then computing lens thickness by subtracting the determined depth from the local instrument elevation above sea level.

Three techniques were chosen for evaluation in Truk because of their relative simplicity and portability in a form suitable for sounding to about 50 m depth. The techniques are Direct Current (DC) Schlumberger sounding, Max/Min (slingram) electromagnetic (EM) profiling, and Very Low Frequency (VLF) EM profiling. The equipment for each technique can be carried and operated by two people and can be transported between islands with the two operators in a 6 m (18 ft) boat.

Each of the techniques measures the subsurface earth resistivity by causing electric currents to flow within the earth. Electric current is injected directly into the earth by means of two electrodes implanted in the earth for

the DC Schlumberger sounding method. Current is induced in the earth indirectly by distant transmitters for the VLF technique and by a small local loop antenna in the Max/Min technique. Resistivity can be measured by the magnitude of the currents which are allowed to flow in the subsurface and by how that magnitude changes when some parameter of the technique is changed (electrode spacing for DC Schlumberger and frequency for Max/Min). Application details of each of the techniques are contained in the appendices with listings of the data and interpretations.

Interpretation of the electromagnetic and DC data are performed here by a nonlinear least squares computer program which finds the horizontally-layered resistivity model whose response best fits the data (see Appendices B and C). The interpretative models used for data in this report include layers whose resistivities are either constant or transitional between adjacent constant-resistivity layers. A resistivity that varies smoothly with depth can closely approximate the increase in salinity with depth which is characteristic of the transition zone between fresh and saline water. Including a transitional layer in the resistivity model is necessary for attempting to model the depth and thickness of the transition zone in the geohydrologic model.

Preliminary studies with synthetic sounding data (theoretically calculated from a known model) show that transitional layers are directly detectable by surface electrical methods if the transitional layer is thick compared to its depth, the smallest detectable thickness being related to the average error in the data. Perfect data can be used to resolve a transitional layer that is at least one-half as thick as its depth. If the average error is 0.4% for Max/Min data or about 0.3% for DC sounding data, then the transitional layer must be thicker than its depth to be resolved. If a resistivity model which includes a transitional layer cannot fit the data better than a model without such a layer, then the later model is chosen for interpretation (because it is simpler and the added complexity of a transitional layer is not justified). For this case, the transition zone is modelled as an abrupt change between two layers of constant resistivity. The synthetic sounding inversions show that, in this case, the abrupt change in model resistivity is located approximately at the middle of the transitional layer for Max/Min data and near the top of the transitional layer for Schlumberger data.

The data errors which might mask the existence of a transitional layer can be due to a number of causes. Major sources of error are distortions caused by pipes, fences, and large metal structures, operational errors (mismeasured electrode or loop spacings), telluric noise, and deviations of the real earth from interpretational assumptions such as horizontal and planar layer boundaries and homogeneous layer resistivities. Even moderate data errors can mask detail in the data that might be useable for resolving a transition zone. Examples of this will be discussed with the Pis island survey.

ELECTRICAL GEOPHYSICAL RESULTS

The reconnaissance period allowed work on three high islands and one low island (Figure 1). The three high islands were Moen, Dublon, and Fefan in the eastern part of the Truk lagoon. The one low island was Pis located to the north of Moen.

MOEN

Six Schlumberger soundings were obtained near Mwan, west Moen and Nemwan on east Moen (Figure 2a). The soundings near Mwan (soundings 1, 2, and 3 in Figure 2b) showed that the zone of weathered volcanics which mantles almost all Moen has a resistivity of between 9 and 26 ohm-m. Each sounding suggests a more resistive basement at about 30 m depth which may be unweathered rock. The soundings near Nemwan (nos. 4, 5, and 6) showed moderate resistivities (44 to 63 ohm-m) at the surface with resistivities greater than 250 ohm-m below a depth of 4 m (Appendix C). The soundings suggest that there is deep (about 30 m) weathering at Mwan and shallow (about 4 m) weathering at Nemwan.

VLF measurements were made at Mwan, Epinup, and the Wichen River valley. VLF Apparent resistivities at the location of DC sounding 1 near Mwan ranged between 8 and 25 ohm-m with phases of approximately 45°. Measurements were also made around a dug well at the edge of a marsh near the town of Epinup, southeast Moen. Apparent resistivity values clustered around 15 ohm-m and phase between 45°-50° with one reading of 70 ohm-m. Measurements at Wichen River were organized along a profile starting at a well in the water and moving perpendicularly away from the stream. Apparent resistivities were 170 ohm-m at the well dropping immediately to 10-20 ohm-m away from the river. With low resistivities rarely exceeding 20 ohm-m, penetration would probably not be greater than about 5 m making VLF measurements useless in determining local weathering conditions. In general, the VLF apparent resistivity values confirm the resistivity values interpreted for the weathered material from the Schlumberger soundings.

DUBLON

Five DC Schlumberger soundings were obtained in the towns of Roro and Nechap on Dublon island (Figure 3a). Soundings 7 through 10 were located along a road through Roro on the eastern side of the island. The geoelectric cross-section obtained (Figure 3b) shows a 2-4 m thick zone at the surface having a resistivity of 80-730 ohm-m. Immediately below this is a thick zone having a resistivity of 15-42 ohm-m, indicating deep weathering. Sounding 7 on the north end of the profile shows a low-resistivity layer about 6 m below sea level possibly representing seawater intrusion. Sounding 10 on the south end of the profile shows a very resistive (>100 ohm-m) basement about 3 m below sea level.

Comparison of the water depths in wells near the geoelectric cross section with the electrical results suggests that the top of the second zone of 15-42 ohm-m represents the water table within the weathered zone because both water in wells and the top of the second geoelectric zone occur 2-4 m below the ground surface. The deep resistive basement apparent at the south end of the profile might be unweathered rock at the base of the weathered material exposed at the ground surface.

One DC Schlumberger sounding between Chun and Nechap on the western side of Dublon shows 21 m of 14-21 ohm-m sediment over a more resistive basement which may be unweathered rock. VLF measurements in the vicinity of the Schlumberger sounding were 15-20 ohm-m in apparent resistivity and 20°-35° in phase. As in Moen, the VLF is only penetrating about 5 m, but the apparent resistivity values agree closely with those interpreted for surface sediment from the Schlumberger sounding.

FEFAN

Two DC Schlumberger soundings were obtained at Messa on the eastern side of Fefan (Figure 4). Sounding 12, situated near a freshwater well, yielded similar results to those seen in Roro, Dublon (Figure 3B). Surface sediments have a resistivity of 175 ohm-m. The second layer, whose top is at the same depth as the water table, has a resistivity of 14 ohm-m. A resistive basement appears 11 m below the surface. Farther inland, sounding 13, located at the edge of the coastal plain, determined the resistive basement to be only 3 m deep. These soundings suggest that it would be possible to trace unweathered

rock beneath the sediments of coastal plains.

Three VLF measurements were taken near wells in Ewes, Kikku, and Fein (Figure 4). In Ewes, the apparent resistivity was 10 ohm-m near a flowing spring. In Kikku, the apparent resistivity was 140 ohm-m near a dry well formerly fed by a spring. Near an old well in Fein, the apparent resistivities were 10 and 20 ohm-m. Each phase determination was poor, but appeared to be about 35° to 40°.

PIS

The most extensive survey was done on Pis, one of the outer islands composed of coralline debris. Two electromagnetic sounding profiles (Figure 5) were run across the island from the lagoon side (south) to the ocean side (north). The Max/Min data were first modelled as due to a two-layer earth with the second layer, representing seawater-saturated sediments below the fresh water lens, being more conductive than the first. The data were also modelled as due to a three-layer earth with the third layer being more conductive than the first and the second layer having a resistivity which was transitional between the first and third layer resistivities. The transition was modelled as a linear change in conductivity with depth to approximate a linear change in salinity within the transition zone. The results of interpretation (Figure 6) show the middle of the transition zone between 3 and 9 m below the ground surface. The middle of the transition zone is used as the marker interface here because the transition zone was not always detected, i.e. the transition zone was thin with respect to its depth and its signal in the data was masked by other effects.

Beneath profile 2, the interface is deeper on the lagoon side (D') and becomes shallower towards the ocean side (D). Beneath profile 1 (C-C'), the interface is shallower in the middle of the island, and appears deeper towards each coast. The resistivity of the seawater-saturated island matrix was about 0.8 ohm-m. The resistivity of the first geoelectric layer, representing sediments above the transition zone, was in the range of 40 to 150 ohm-m.

Five DC soundings were located along the Max/Min profiles for comparison (Figure 5 and 6). Each set of sounding data was fit with a four- or five-layer model. The deepest three layers represented fresh water-saturated sediments, a linear transition zone, and seawater-saturated sediments. The one or two layers above these three represented unsaturated sedimentary layers. Two soundings (15 and 17) distinctly resolved a 2-3 m thick transition zone and a very thin layer which might represent fresh-water saturated sediments. The transition zone was too thin to resolve (relative to the error in the soundings) in the other three soundings (14, 16, and 18).

The depth to the marker horizon (the middle of the transitional layer or the top of the basement conductor if no transitional layer was resolved) as determined by DC soundings is always less than the depth determined by Max/Min sounding. The discrepancy is to be expected owing to the different sensitivities of the EM and DC techniques (Raiche and others, 1985). EM is very sensitive to conductive material and fairly insensitive to resistive material. On the other hand, DC is sensitive to both resistive and conductive material, but can underestimate depths due to equivalence of thin, intermediate layers or anisotropy of intermediate layers. The synthetic sounding study discussed earlier in this report has already shown that if a transition zone must be modelled as an abrupt change in resistivity, then that interface will be at the top of the transition zone for Schlumberger data and near the middle for Max/Min data. Depths to the basement conductor under Pis island determined from Max/Min data are smooth and consistent from one position in a profile line to another, whereas the depths to a specific horizon in the Schlumberger sounding interpretations can vary abruptly. It appears that the Max/Min results are the more consistent. Superior interpretation could probably be achieved by jointly inverting both Schlumberger and Max/Min data.

EVALUATION OF THE TECHNIQUES AND RECOMMENDATIONS

For low islands such as Pis, Max/Min profiling seems to work well for determining depth to the seawater-saturated sediments (or the middle of the transition zone). The only geohydrologic data available with which to compare the geoelectric results are the chloride contents of water in dug wells along the two profiles on Pis (noted on Figure 6a and b). In a crude sense, these salinities increase where the geoelectric results show a decrease in depth to the middle of the transition zone; however, the data are not extensive enough to make the comparison definitive.

The environmental factors which make the application of EM profiling techniques ideal are the large resistivity contrast between seawater- and fresh water-saturated sediments and the absence of good conductors above the transition zone. EM techniques are relatively insensitive to the higher resistivities within and above the transition zone, but are much more sensitive to the resistivity and depth to the conductive material within and below the transition zone than are DC techniques. DC Schlumberger can also be used, but the depth determinations are more ambiguous. DC techniques are sensitive to the higher resistivities within and above the transition zone. When the resistivity structure above the interface involves more than one resistivity (the usual case), both resistivities and layer thicknesses become

more difficult to interpret. The VLF technique is not precise enough at large distances from the transmitters to make the depth determination. The close proximity to ocean can distort the VLF readings.

For the high islands, DC Schlumberger sounding can be used to determine the thickness of either coastal plain sediments or weathered volcanics above impermeable, unweathered volcanics. Lack of knowledge about the aquifer in the areas in which geoelectric data were obtained prevents any evaluation of these techniques for aquifer discrimination; however, it appeared in Mwan, Moen and Roro, Dublon that water-saturation reduced the resistivity of the weathered volcanics and alluvium by a factor of ten. This contrast would suggest the possibility of mapping the water surface directly. Max/Min with a 61 m spacing would be unable to penetrate more than 15 m and VLF would be unable to penetrate more than 5 m of 20 ohm-m sediment, severely limiting their utility in the high volcanic islands.

Portable versions of the Max/Min EM profiling and DC Schlumberger sounding equipment sets would allow ground water exploration in the broadest range of island environments. Max/Min profiling with a few Schlumberger soundings is most suitable for low island environments; DC Schlumberger sounding is most suitable for high island environments.

APPENDIX A: VLF Data

The VLF data were taken with a Geonics EM16R unit using stations NWC (22.3 kHz) located at North West Cape, Australia and NPM (23.4 kHz) located at Lualualei, O'ahu, Hawai'i. The apparent resistivity (ρ_{oa}) and phase angle (phase) of the VLF electromagnetic field were measured. Signals appeared to be very weak, making accurate measurement of these quantities difficult. The estimated error of the values listed in Table I is greater than 20 percent.

Table IV. VLF Field Data

location	ρ_{oa} ohm-m	phase degrees	comments
Mwan, Moen	20	55	above road, sdg 1
	8	35	on road
	10	50	50 m below road
	20	45	80 m below road
	25	45	110 m below road
Epinup, Moen	15	52	immed. east of well
	15	54	immed. west of well
	70	50	50 m west of well
	16	50	15 m from well towards marsh
	14	45	100 m west of well
Wichen River, Moen	170	40	at well in river
	20	45	east bank
	14	50	west bank
	10	50	west bank, 25 m from river
	10	50	west bank, 40 m from river
	15	50	west bank, 100 m from river
Nechap, Dublon	40	35	Nechinipwa well
	15	35	at sounding 11
	15	35	100 m inland
	20	20	200 m inland
Ewes, Fefan	10	40	on rise above Sikar well
Kikku, Fefan	140	35	15 m S of dry well above Kikku
Fein, Fefan	10	40	japanese well
	20	40	200 m towards ocean

APPENDIX B: Loop-loop EM Data

All loop-loop EM data were taken in the horizontal, coplanar loop mode (Parasnis, 1979) with the transmitter and receiver loops separated 61 m (200 ft). The in-phase or real (R) portion and the out-of-phase or imaginary (I) portion of the loop coupling at each of five frequencies - 222, 444, 888, 1777, 3555 Hz were measured. The data units are in percent of the coupling that would be observed in the absence of all conductive material. Note that the R measurement is actually equal to the real portion of the coupling minus 100 percent and that R values significantly greater than 35 are theoretically impossible for any horizontally-layered earth model and are indicative of distortion. Values are read on three different scales and therefore provide three different levels of precision. Values between plus and minus 4 percent can be read to the nearest 0.1 percent, values between plus and minus 25 percent can be read to the nearest 0.5 percent, and values between plus and minus 100 percent can be read to the nearest 2.5 percent.

Interpretation was done with the aid of computer program MARQLOOPS_HP, an enhanced, Hewlett-Packard 9826 BASIC 2.1 version of program MARQLOOPS (Anderson, 1979b), which finds the best-fitting, horizontally-layered earth model for a given loop-loop EM profile data set. Input to the program consists of the data set, the number of layers, and a first guess at the resistivities and thicknesses of those layers. Layers may have constant or transitional resistivities. A transitional layer may vary linearly in either resistivity or conductivity. The program can automatically adjust the model for possible errors in loop spacing by varying the loop spacing as if it were another model parameter.

The interpretation for data sets 1-1 through 1-6 (going south to north) are plotted in Figure 6a as profile 1. The interpretations for data sets 2-1 through 2-4 (also going south to north) are plotted in Figure 6b.

Table V. Loop-Loop EM Field Data

No.	Frequency:222		444		888		1777		3555 Hz	
	R	I	R	I	R	I	R	I	R	I
1-1	35	2	30	-28	-3	-42	-28	-29	-43	-24
1-2	34	0.4	27	-26	-3	-48	-33	-42	-52	-30
1-3	27	-7	17	-35	-11	-48	-40	-41	-57	-29
1-4	25	-10.5	12	-38	-18	-49	-45	-39	-62	-25
1-5	26	-9	13.5	-39	-18	-52	-47	-41	-63	-27
1-6	24	-7	13	-35	-15	-47	-43	-38	-58	-26
2-1	30	-7	22	-30	-11	-45	-35	-36	-50	-23
2-2	27	-11	12.5	-39	-26	-49	-46	-38	-63	-26
2-3	30	-15	12.5	-48	-22	-58	-56	-43	-74	-26
2-4	24	-24	-2.5	-58	-43	-59	-69	-34	-76	-19

APPENDIX C: Schlumberger Sounding Data and Computer Interpretations

A resistivity sounding consists of a series of apparent resistivity measurements taken at several different electrode positions created by expanding four electrodes symmetrically about a central point (two on each side), preferably along a straight line. Electric current is forced into the ground through the outer two electrodes (current electrodes) and the voltage produced by that current is measured between the inner two electrodes (potential electrodes). Larger current electrode separations generally force deeper current penetration; thus, it is possible to influence the depth of investigation by varying the current electrode separation. For the Schlumberger electrode array, the potential electrodes are placed no farther apart than one-fifth the separation between the current electrodes.

Data anomalies due to local lateral inhomogeneities can sometimes be recognized by moving either the potential electrodes or the current electrodes between readings, but not both at the same time. In practice, the potential electrodes are moved once for every four or five current electrode moves. Apparent resistivity values obtained for the same current electrode separation with two different potential electrode separations are almost always slightly different due to small inhomogeneities around the electrodes and/or the use of homogeneous earth potential variations to reduce real, nonhomogeneous earth potential variations; this difference must be removed to give an unbroken data set for quantitative interpretation. The differences are removed by holding a data segment, made with a particular potential electrode separation, fixed and shifting the remaining segments up or down so that the end points match adjacent segments. Many conventions can be used for deciding to what base segment the rest will be shifted. For most sounding data sets, all segments are shifted to the segment measured with the largest potential electrode spacing.

Computer program MARQDCLAG_HP, an enhanced Hewlett-Packard 9826 BASIC version of MARQDCLAG (Anderson, 1979a), offers an automatic means by which sounding data sets, like those obtained in the course of this study, can be inverted to their best-fitting horizontally-layered model parameters - resistivities and thickness. The layers in the model may either have a uniform resistivity or a resistivity which varies from the resistivity of the layer above it to the resistivity of the layer below. The resistivity can be selected to vary linearly in either resistivity or conductivity. Of course, approximate matching can be done by manually comparing the sounding data to theoretical curves in a standard album; however, the computer inversion offers several advantages, including speed, automation, and estimation of parameter resolution.

MARQDCLAG_HP automatically minimizes the following quantity:

$$PHI = \sum_{i=1}^N \left[\frac{y_i - f(x_i)}{e_i} \right]^2$$

where N is the number of data in the sounding data set,

x_i is the i th current electrode spacing,
 y_i is the measured apparent resistivity measured at x_i ,
 e_i is the apparent resistivity measurement error
 (default = $y_i / 100$), and
 $f(x)$ is the theoretical apparent resistivity calculated from the earth model.

Along with the sounding data set, the program requires a starting guess of all model parameters.

The number of layers cannot be automatically varied by the program so it is a common practice to invert each sounding data set for several models, each having a different number of layers. The best-fitting model is chosen to be the one which minimizes the following quantity, called the reduced chi-squared statistic:

$$REDUCED\ CHI-SQUARED = PHI / (N - 1 - K)$$

where K is the number of parameters in the model being fit to the data. In general applications, $K = 2 * m - 1$ where m is the number of layers in the theoretical model and * denotes multiplication.

During the inversions of the sounding data sets, the natural logarithm of the model parameters, rather than the parameters themselves, were manipulated to avoid the possibility of negative resistivities or thicknesses and to more accurately reflect the logarithmic resolution of these values. The values and their error estimates are converted back to normal units before being output by the program. A detailed description of the headings and identifying terms used in the program output listed in this Appendix follows:

X electrode spacing equal to half the distance between the two current electrodes, meters,

OBSERVED shifted observed apparent resistivity values, ohm-meters,
PREDICTED apparent resistivity values predicted or calculated from
 the best-fitting model parameters,
%RESIDUALS $(\text{OBSERVED}-\text{PREDICTED}) \cdot 100,$
 $\frac{2}{}$
WEIGHT FN $1/(\text{error})^2$, where error is normally OBSERVED/100,
CORRELATION MATRIX estimates of the correlation between each of the model
 parameters and any other parameters of this particular
 model. One values down the diagonal indicate that each
 parameter is 100% positively correlated with itself
 (expected). Numbers between +1 and -1 off the diagonal
 indicate the degree of correlation between each pair of
 parameters. A correlation of zero indicates no
 correlation. A correlation of +1 or -1 indicate perfect
 positive or negative correlation, respectively,
REDUCED CHI-SQUARED the statistic corresponding to the previously-defined
 formula,

Two different versions of printouts are included in this appendix. Most indicate the best-fitting model under the following headings:

B-SD $\exp^1(\text{PARAMETER}-\text{ERROR}),$
B $\exp(\text{PARAMETER}),$
B+SD $\exp(\text{PARAMETER}+\text{ERROR}),$

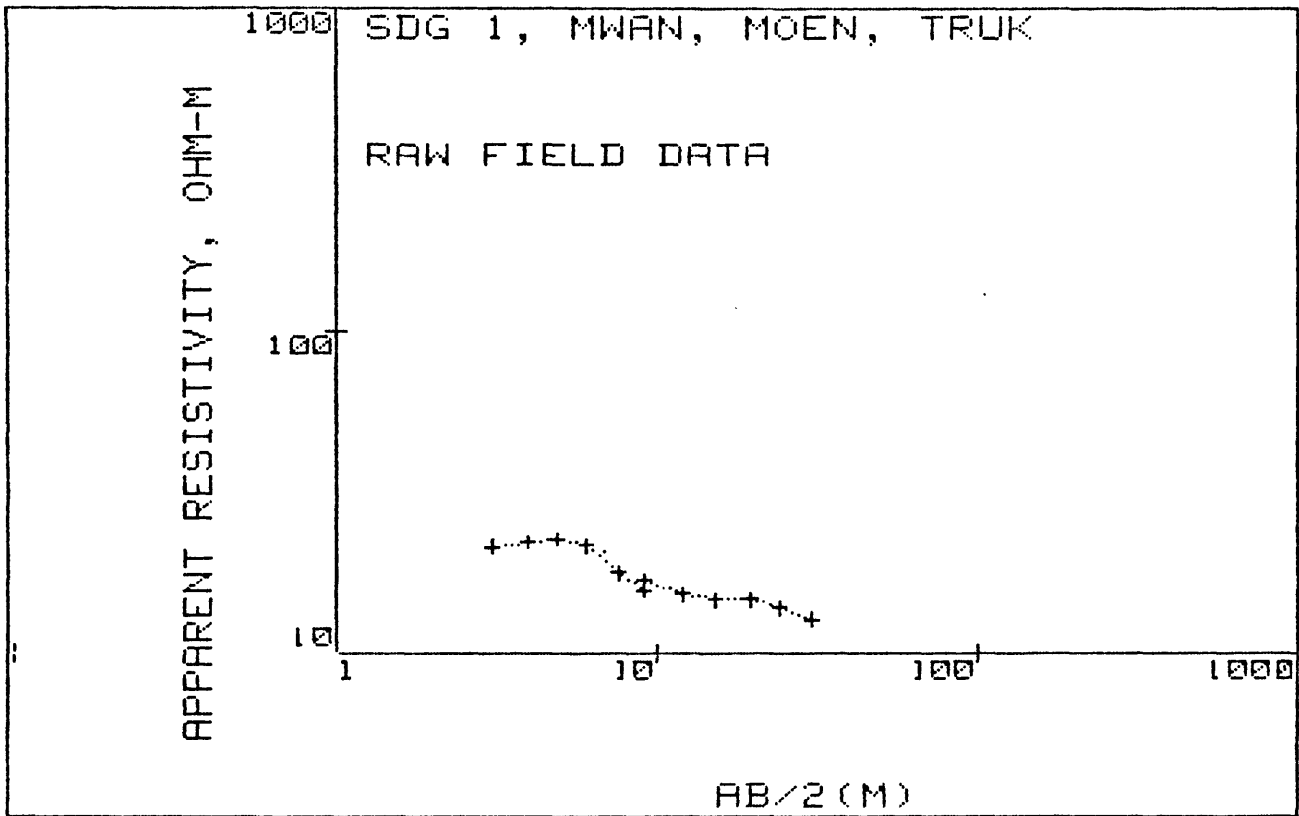
FINAL UNSCALED PARAMETERS:

RESISTIVITY resistivity of layer i, in ohm-meters,
DEPTH depth from surface to bottom of layer i, in meters.

¹
 $\exp(x)$ represents e, the base of the natural logarithms, raised to the x power.

The few inversion printouts at the end of this appendix (for sounding data obtained on Pis island) indicate the best-fitting model under the following different headings:

- RESISTIVITY in ohm-m, three columns with the left- and right-most column indicating lower and upper estimated bounds on the best-fitting resistivity in the middle column. Asterisks indicate that resistivity was not allowed to vary during the inversion. Blanks in the right-most column indicate an upper bound that is essentially infinite (no upper bound). Negative resistivities indicate transitional layers. A resistivity of -1 indicates a linear resistivity and -2 indicates a linear conductivity.
- THICKNESS in meters, three columns with the left- and right-most column indicating lower and upper estimated bounds on the best-fitting thickness in the middle column. Asterisks indicate that thickness wasnot allowed to vary during the inversion. Blanks in the right-most column indicate an upper bound that is essentially infinite (no upper bound).
- DEPTH in meters, depth to the upper surface of that layer from ground surface.
- ELEV in meters, elevation of the upper surface of that layer from sea level if the sounding elevation has been entered, or from ground surface (in this case $ELEV = - DEPTH$).



AB/2 (M)	APP. RHO
3.0	21.4
4.0	22.1
4.9	22.5
6.1	21.5
7.6	17.8
9.1	15.6
9.1	16.8
12.2	15.2
15.2	14.7
19.8	14.7
24.4	13.8
30.5	12.7

MARQUARDT STATISTICS: SDG 1, MWAN, MOEN, TRUK

	X	OBSERVED	PREDICTED	%RESIDUALS	WEIGHT FN
1	+3.0480E+00	+2.3046E+01	+2.4643E+01	-6.9281E+00	+5.3772E-01
2	+3.9624E+00	+2.3800E+01	+2.3721E+01	+3.3072E-01	+5.0420E-01
3	+4.8768E+00	+2.4231E+01	+2.2629E+01	+6.6086E+00	+4.8643E-01
4	+6.0960E+00	+2.3154E+01	+2.1098E+01	+8.8792E+00	+5.3273E-01
5	+7.6200E+00	+1.9169E+01	+1.9319E+01	-7.8274E-01	+7.7722E-01
6	+9.1440E+00	+1.6800E+01	+1.7844E+01	-6.2148E+00	+1.0119E+00
7	+1.2192E+01	+1.5200E+01	+1.5822E+01	-4.0952E+00	+1.2361E+00
8	+1.5240E+01	+1.4700E+01	+1.4685E+01	+1.0359E-01	+1.3217E+00
9	+1.9812E+01	+1.4700E+01	+1.3829E+01	+5.9222E+00	+1.3217E+00
10	+2.4384E+01	+1.3800E+01	+1.3429E+01	+2.6890E+00	+1.4997E+00
11	+3.0480E+01	+1.2700E+01	+1.3168E+01	-3.6848E+00	+1.7707E+00

CORRELATION MATRIX:

	1	2	3
1	+1.00	+0.40	-0.77
2	+0.40	+1.00	-0.72
3	-0.77	-0.72	+1.00

REDUCED CHI-SQUARED=40.36
PHI=282.52

DCLAG: ***** END *****

SDG 1, MWAN, MOEN, TRUK

COORDINATES: 0 0

ELEVATION : 0

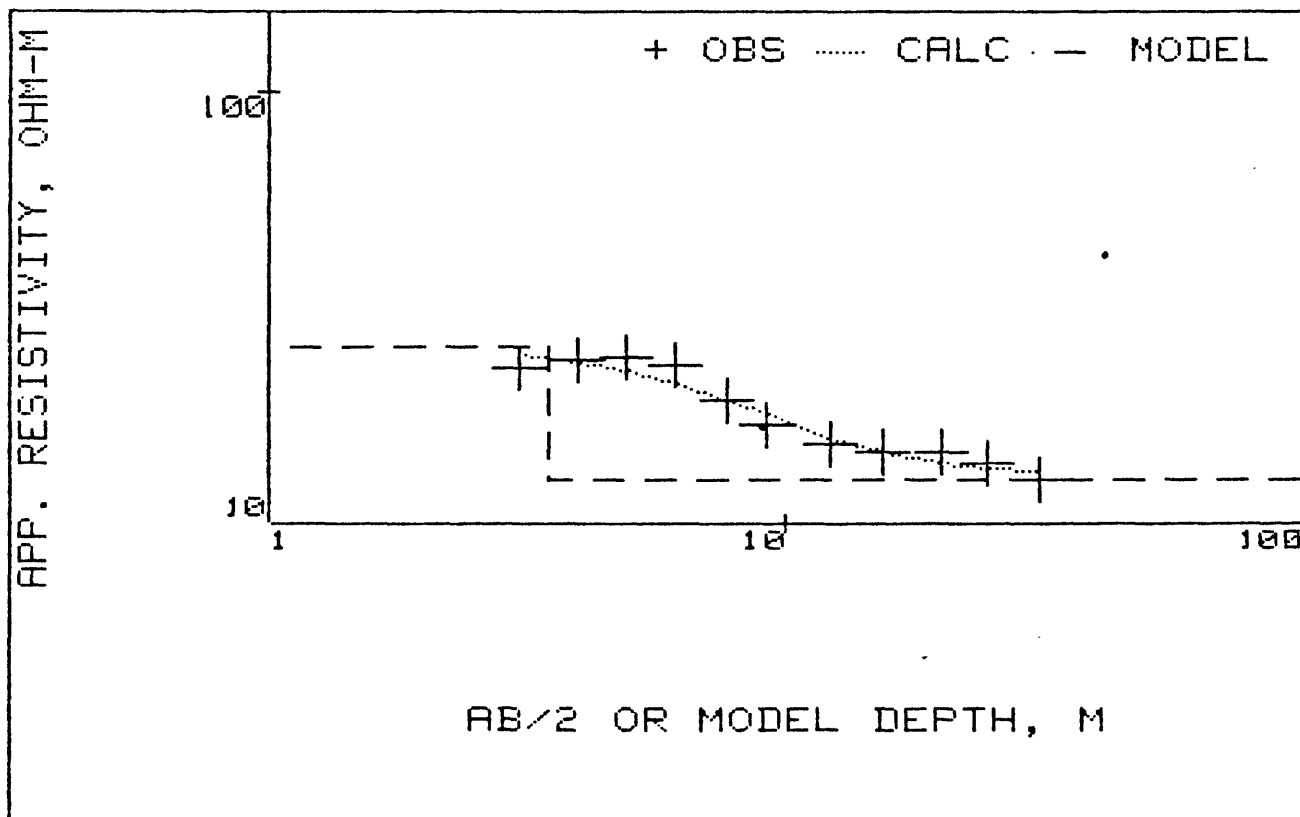
AZIMUTH :

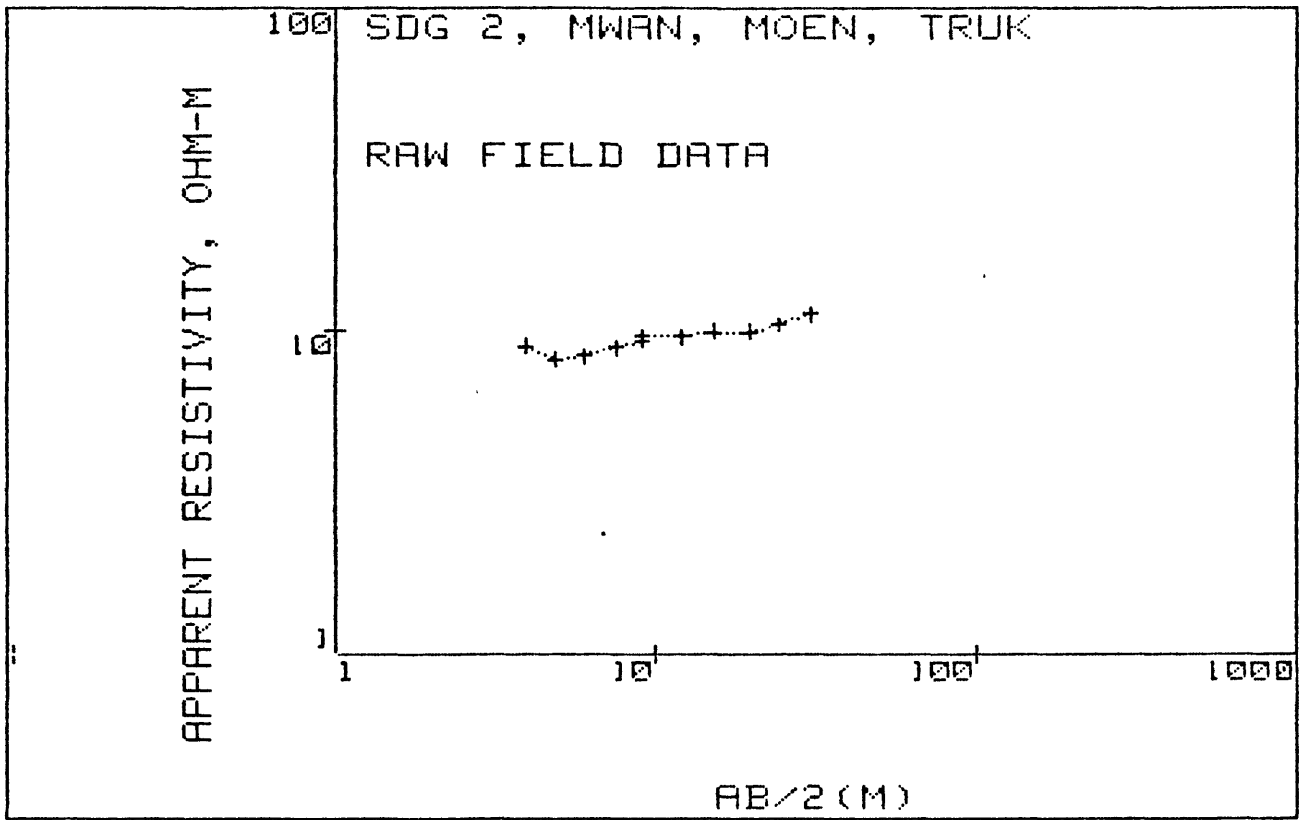
B-SD	B	B+SD
1.845E+001	2.571E+001	3.582E+001
9.682E+000	1.276E+001	1.681E+001
1.441E+000	3.482E+000	8.413E+000

FINAL UNSCALED PARAMETERS--
(* denotes fixed value)

	RESISTIVITY	DEPTH
1	2.57071694E+01	1 2.570717E+01
2	1.27562959E+01	2 1.275630E+01
3	3.48165255E+00	1 3.481653E+00

SDG 1, MWAN, MOEN, TRUK





AB/2 (M)	APP. RHO
4.0	8.9
4.9	8.1
6.1	8.3
7.6	8.8
9.1	9.2
9.1	9.5
12.2	9.5
15.2	9.8
19.8	9.8
24.4	10.3
30.5	11.1

MARQUARDT STATISTICS: SDG 2, MWAN, MOEN, TRUK

	X	OBSERVED	PREDICTED	%RESIDUALS	WEIGHT FN
1	+3.9624E+00	+9.1902E+00	+8.7534E+00	+4.7535E+00	+1.0535E+00
2	+4.8768E+00	+8.3641E+00	+8.7899E+00	-5.0909E+00	+1.2719E+00
3	+6.0960E+00	+8.5707E+00	+8.8573E+00	-3.3451E+00	+1.2113E+00
4	+7.6200E+00	+9.0870E+00	+8.9690E+00	+1.2979E+00	+1.0776E+00
5	+9.1440E+00	+9.5000E+00	+9.1047E+00	+4.1615E+00	+9.8592E-01
6	+1.2192E+01	+9.5000E+00	+9.4142E+00	+9.0307E-01	+9.8592E-01
7	+1.5240E+01	+9.8000E+00	+9.7283E+00	+7.3130E-01	+9.2648E-01
8	+1.9812E+01	+9.8000E+00	+1.0143E+01	-3.5037E+00	+9.2648E-01
9	+2.4384E+01	+1.0300E+01	+1.0471E+01	-1.6569E+00	+8.3872E-01
10	+3.0480E+01	+1.1100E+01	+1.0791E+01	+2.7877E+00	+7.2218E-01

CORRELATION MATRIX:

	1	2	3
1	+1.00	+.50	+.71
2	+.50	+1.00	+.92
3	+.71	+.92	+1.00

REDUCED CHI-SQUARED=17.14
 PHI=102.85

DCLAG: ***** END *****

SDG 2, MWAN, MOEN, TRUK

COORDINATES: 0 0

ELEVATION : 0

AZIMUTH :

E-SD	B	B+SD
6.414E+000	8.706E+000	1.182E+001
3.748E+000	1.181E+001	3.721E+001
7.266E-002	7.353E+000	7.442E+002

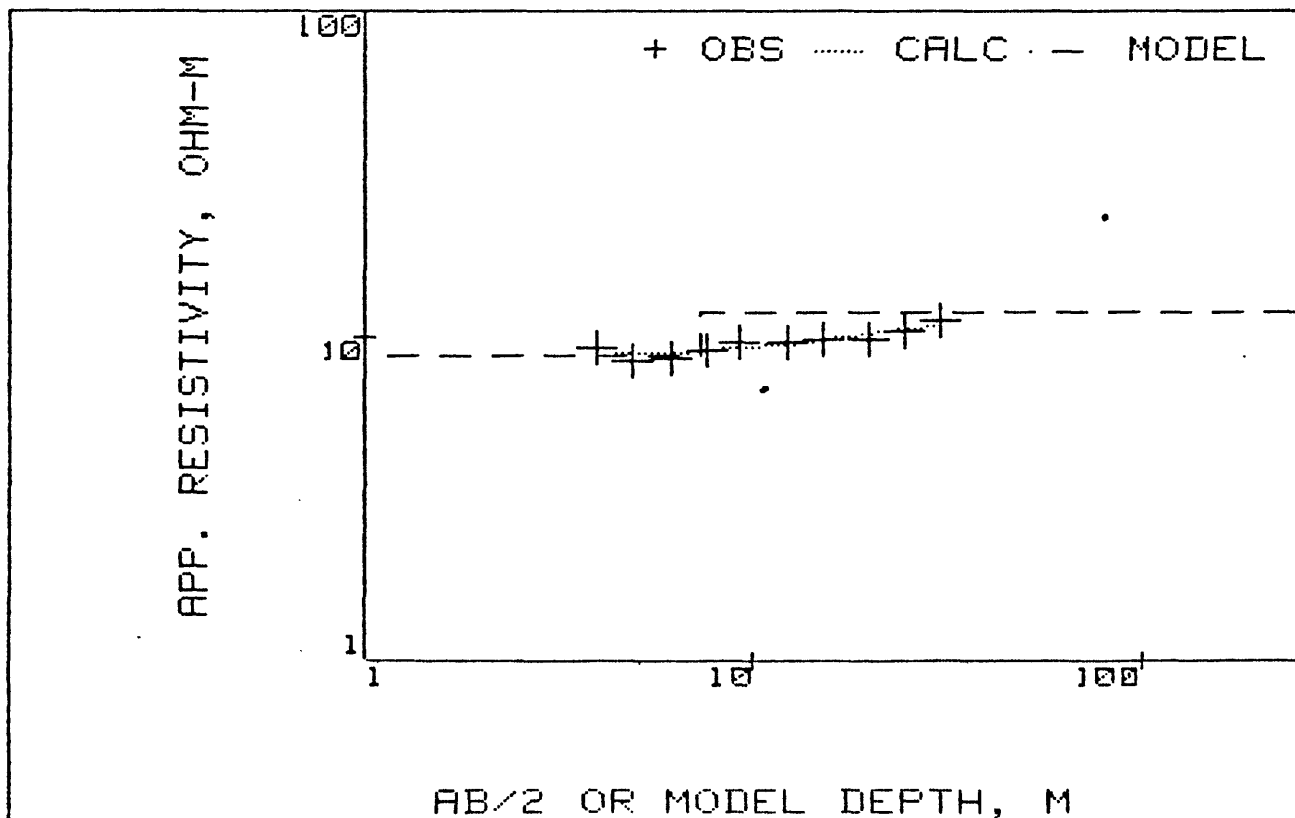
FINAL UNSCALED PARAMETERS--
(* denotes fixed value)

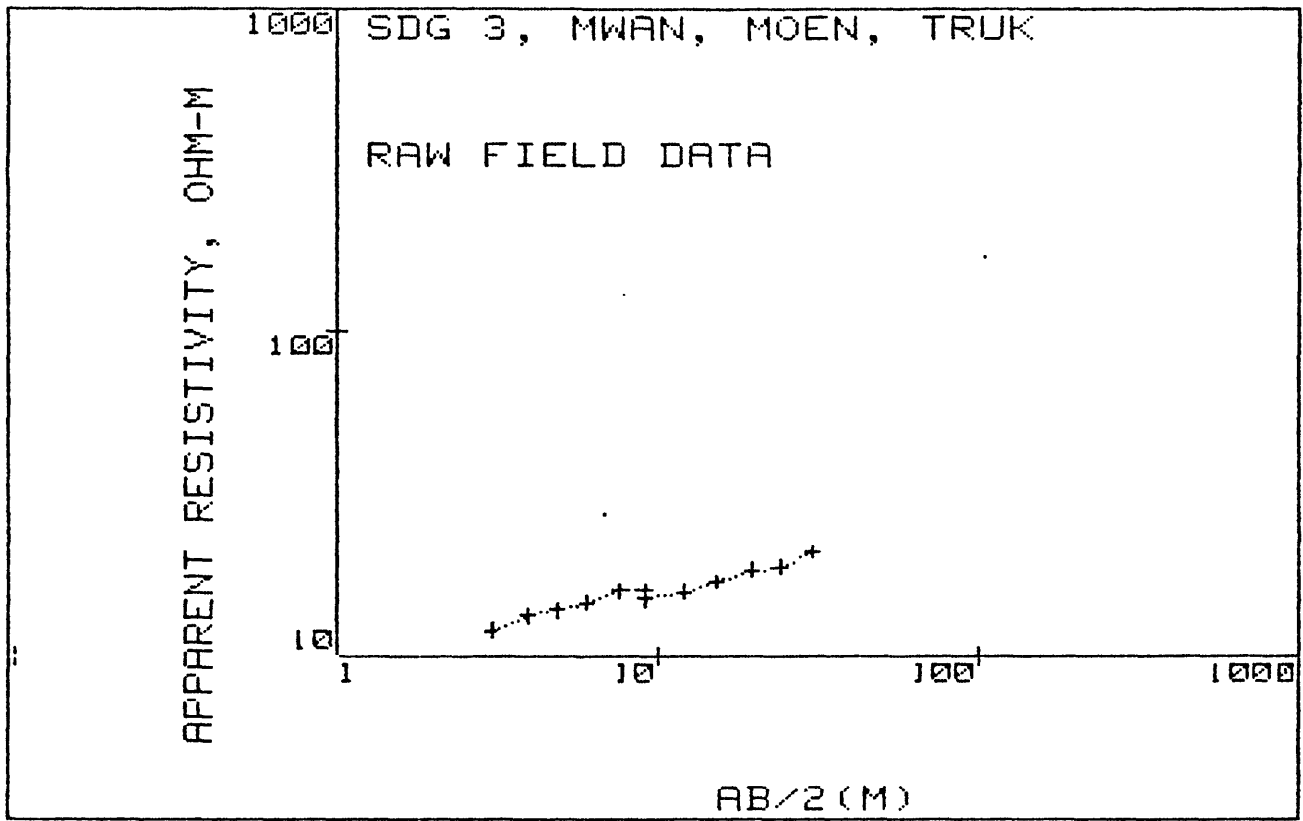
RESISTIVITY

DEPTH

1	8.70599642E+00	1	8.705996E+00		
2	1.18091336E+01	2	1.180913E+01		
3	7.35343173E+00			1	7.353432E+00

SDG 2, MWAN, MOEN, TRUK





AB/2 (M)	APP. RHO
3.0	12.0
4.0	13.3
4.9	13.8
6.1	14.6
7.6	15.9
9.1	15.8
9.1	14.9
12.2	15.7
15.2	16.9
19.8	18.3
24.4	18.7
30.5	20.9

MARQUARDT STATISTICS: SDG 3, MWAN, MOEN, TRUK

	X	OBSERVED	PREDICTED	%RESIDUALS	WEIGHT FN
1	+3.0480E+00	+1.1316E+01	+1.1838E+01	-4.6100E+00	+1.7182E+00
2	+3.9624E+00	+1.2542E+01	+1.2235E+01	+2.4481E+00	+1.3988E+00
3	+4.8768E+00	+1.3014E+01	+1.2721E+01	+2.2531E+00	+1.2992E+00
4	+6.0960E+00	+1.3768E+01	+1.3433E+01	+2.4366E+00	+1.1608E+00
5	+7.6200E+00	+1.4994E+01	+1.4322E+01	+4.4857E+00	+9.7871E-01
6	+9.1440E+00	+1.4900E+01	+1.5134E+01	-1.5721E+00	+9.9113E-01
7	+1.2192E+01	+1.5700E+01	+1.6452E+01	-4.7929E+00	+8.9270E-01
8	+1.5240E+01	+1.6900E+01	+1.7414E+01	-3.0394E+00	+7.7043E-01
9	+1.9812E+01	+1.8300E+01	+1.8401E+01	-5.5291E-01	+6.5706E-01
10	+2.4384E+01	+1.8700E+01	+1.9050E+01	-1.8712E+00	+6.2925E-01
11	+3.0480E+01	+2.0900E+01	+1.9612E+01	+6.1609E+00	+5.0375E-01

CORRELATION MATRIX:

	1	2	3
1	+1.00	+.46	+.84
2	+.46	+1.00	+.77
3	+.84	+.77	+1.00

REDUCED CHI-SQUARED=19.26
 PHI=134.83

DCLAG: ***** END *****

SDG 3, MWAN, MOEN, TRUK

COORDINATES: 0 0
ELEVATION : 0
AZIMUTH :

B-SD	B	B+SD
8.243E+000	1.139E+001	1.575E+001
1.512E+001	2.107E+001	2.937E+001
9.878E-001	3.527E+000	1.260E+001

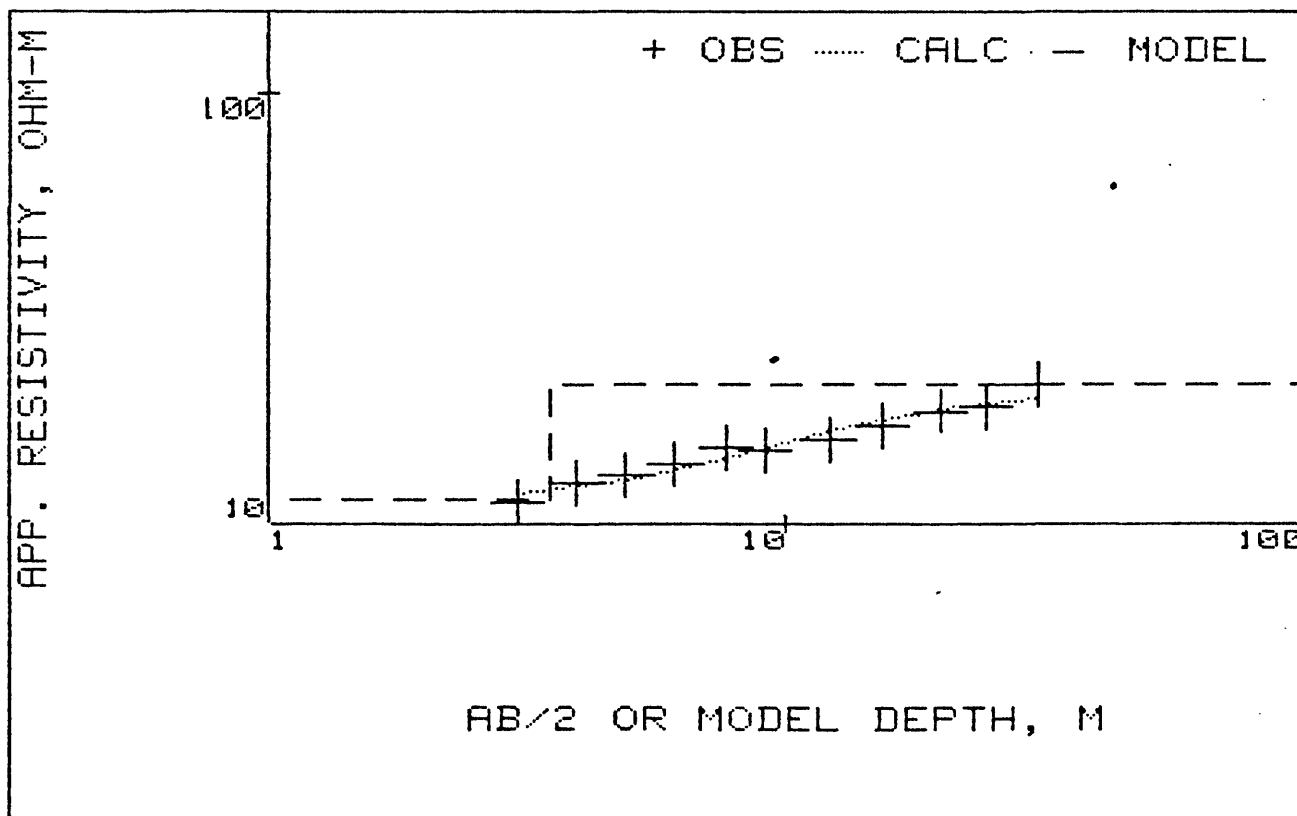
FINAL UNSCALED PARAMETERS-- .
(* denotes fixed value)

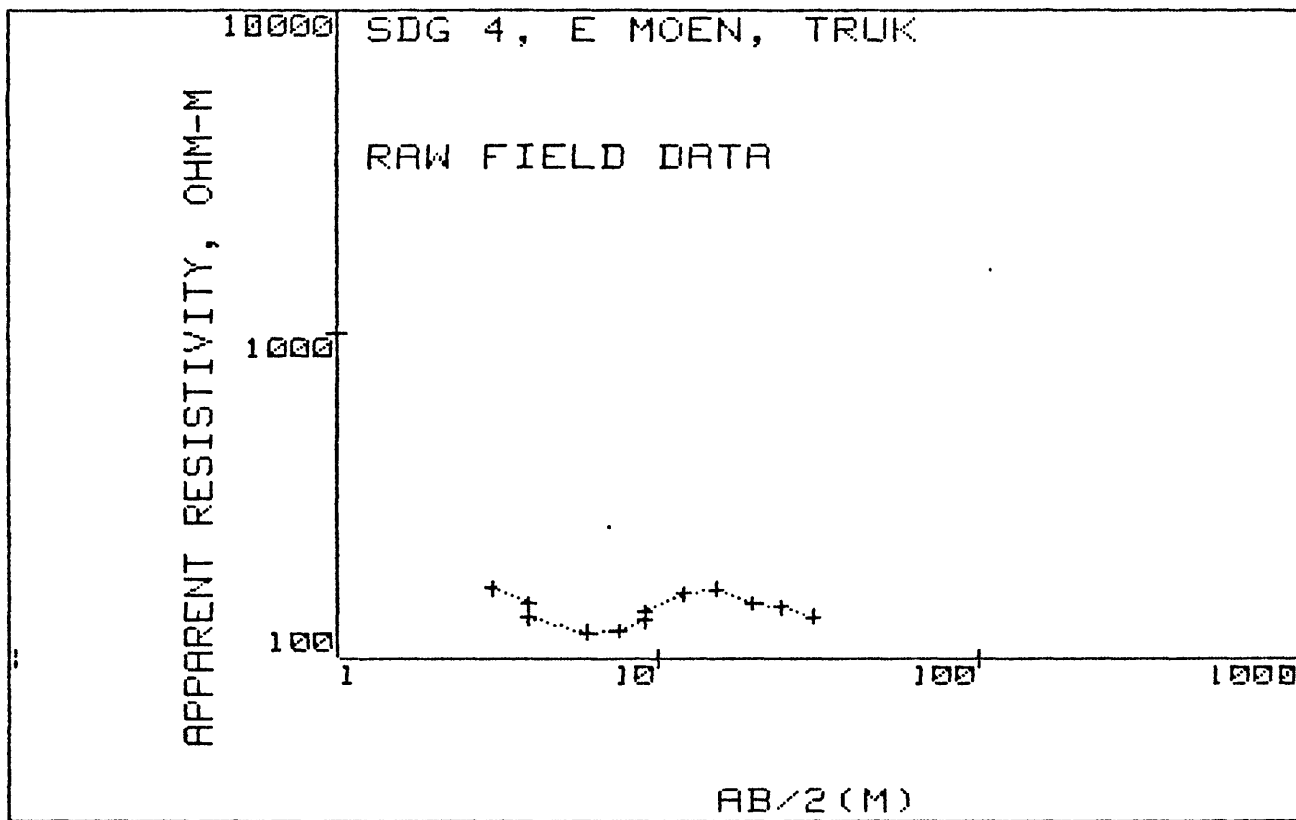
RESISTIVITY

DEPTH

1	1.13933215E+01	1	1.139332E+01	
2	2.10710465E+01	2	2.107105E+01	
3	3.52742381E+00			1 3.527424E+00

SDG 3, MWAN, MOEN, TRUK





AB/2 (M)	APP. RHO
3.0	164.5
4.0	147.3
4.0	133.3
6.1	120.4
7.6	121.9
9.1	130.3
9.1	138.8
12.2	158.1
15.2	164.0
19.8	147.6
24.4	143.6
30.5	135.0

MARQUARDT STATISTICS: SDG 4, E MOEN, TRUK

	X	OBSERVED	PREDICTED	%RESIDUALS	WEIGHT FN
1	+3.0480E+00	+1.5858E+02	+1.5975E+02	-7.4185E-01	+8.1519E-01
2	+3.9624E+00	+1.4200E+02	+1.4020E+02	+1.2656E+00	+1.0167E+00
3	+6.0960E+00	+1.2825E+02	+1.2849E+02	-1.8102E-01	+1.2462E+00
4	+7.6200E+00	+1.2985E+02	+1.3332E+02	-2.6687E+00	+1.2157E+00
5	+9.1440E+00	+1.3880E+02	+1.4007E+02	-9.1564E-01	+1.0640E+00
6	+1.2192E+01	+1.5810E+02	+1.5086E+02	+4.5816E+00	+8.2011E-01
7	+1.5240E+01	+1.6400E+02	+1.5610E+02	+4.8156E+00	+7.6217E-01
8	+1.9812E+01	+1.4760E+02	+1.5550E+02	-5.3554E+00	+9.4095E-01
9	+2.4384E+01	+1.4360E+02	+1.4781E+02	-2.9313E+00	+9.9410E-01
10	+3.0480E+01	+1.3500E+02	+1.3109E+02	+2.8936E+00	+1.1248E+00

CORRELATION MATRIX:

	1	2	3	5	6	7
1	+1.00	+.94	+.76	-.96	+.94	-.84
2	+.94	+1.00	+.90	-1.00	+1.00	-.95
3	+.76	+.90	+1.00	-.87	+.91	-.99
5	-.96	-1.00	-.87	+1.00	-1.00	+.93
6	+.94	+1.00	+.91	-1.00	+1.00	-.96
7	-.84	-.95	-.99	+.93	-.96	+1.00

REDUCED CHI-SQUARED=33.32
 PHI=99.972

DCLAG: ***** END *****

SDG 4, E MOEN, TRUK

COORDINATES: 0 0

ELEVATION : 0

AZIMUTH :

B-SD	B	B+SD
1.074E+002	2.248E+002	4.703E+002
7.333E-008	4.565E+001	2.842E+010
1.392E+002	2.121E+002	3.231E+002
	1.000E+000	
7.420E-002	1.629E+000	3.578E+001
6.308E-011	1.080E+000	1.849E+010
6.805E+000	1.695E+001	4.224E+001

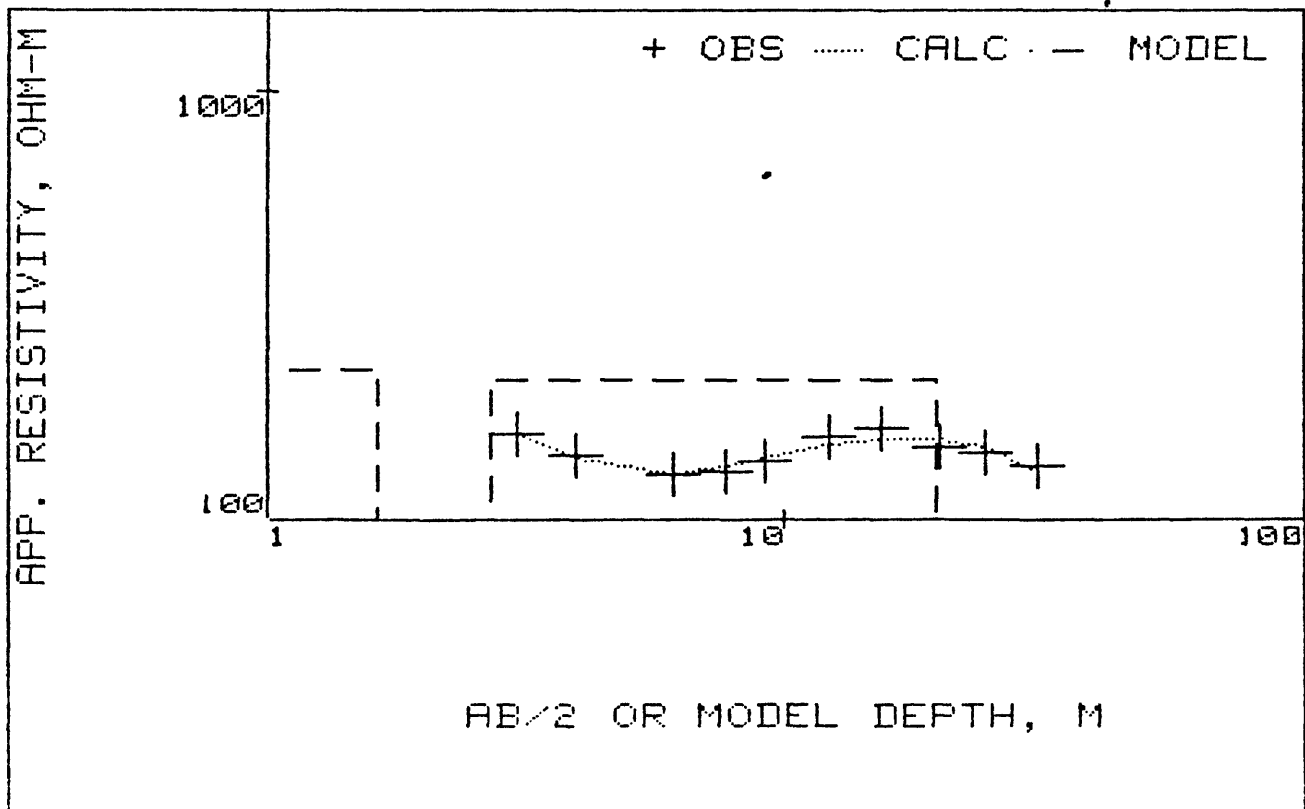
FINAL UNSCALED PARAMETERS--
(* denotes fixed value)

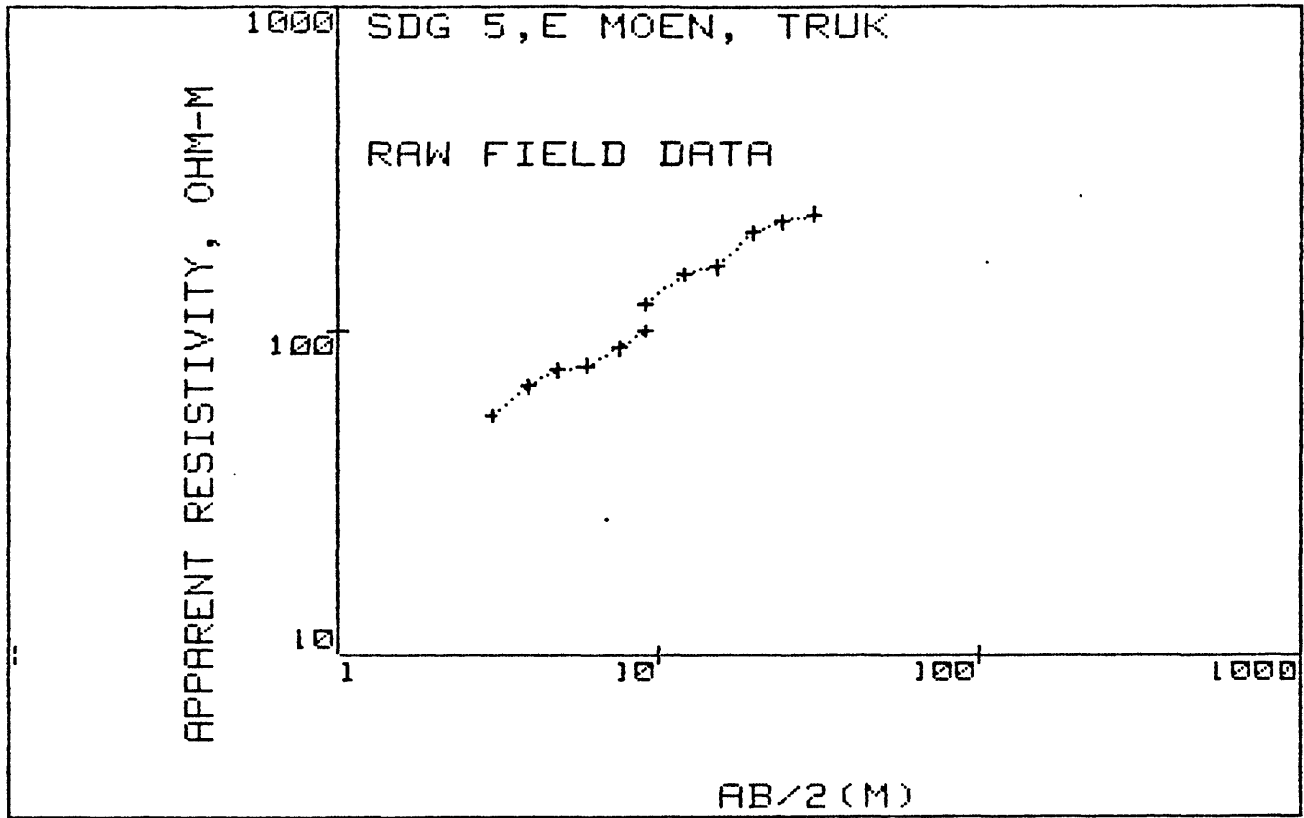
RESISTIVITY

DEPTH

1	2.24765857E+02	1	2.247659E+02		
2	4.56522225E+01	2	4.565222E+01		
3	2.12088036E+02	3	2.120880E+02		
4 *	1.00000000E+00	4	1.000000E+00		
5	1.62932413E+00			1	1.629324E+00
6	1.07997149E+00			2	2.709296E+00
7	1.69542365E+01			3	1.966353E+01

SDG 4, E MOEN, TRUK





AB/2 (M)	APP. RHO
3.0	54.6
4.0	67.2
4.9	75.4
6.1	77.7
7.6	87.6
9.1	99.4
9.1	120.5
12.2	148.8
15.2	156.3
19.8	197.2
24.4	212.8
30.5	224.8

MARQUARDT STATISTICS: SDG 5,E MOEN, TRUK

	X	OBSERVED	PREDICTED	%RESIDUALS	WEIGHT FN
1	+3.0480E+00	+6.6190E+01	+7.0300E+01	-6.2092E+00	+2.7215E+00
2	+3.9624E+00	+8.1465E+01	+7.6599E+01	+5.9723E+00	+1.7966E+00
3	+4.8768E+00	+9.1405E+01	+8.4218E+01	+7.8637E+00	+1.4271E+00
4	+6.0960E+00	+9.4194E+01	+9.5373E+01	-1.2516E+00	+1.3439E+00
5	+7.6200E+00	+1.0620E+02	+1.0950E+02	-3.1097E+00	+1.0573E+00
6	+9.1440E+00	+1.2050E+02	+1.2289E+02	-1.9868E+00	+8.2116E-01
7	+1.2192E+01	+1.4880E+02	+1.4647E+02	+1.5653E+00	+5.3851E-01
8	+1.5240E+01	+1.5630E+02	+1.6603E+02	-6.2244E+00	+4.8807E-01
9	+1.9812E+01	+1.9720E+02	+1.8950E+02	+3.9049E+00	+3.0661E-01
10	+2.4384E+01	+2.1280E+02	+2.0778E+02	+2.3583E+00	+2.6330E-01
11	+3.0480E+01	+2.2480E+02	+2.2648E+02	-7.4600E-01	+2.3594E-01

CORRELATION MATRIX:

	1	2	3
1	+1.00	+0.45	+0.90
2	+0.45	+1.00	+0.73
3	+0.90	+0.73	+1.00

REDUCED CHI-SQUARED=30.54
 PHI=213.8

DCLAG: ***** END *****

SDG 5,E MOEN, TRUK

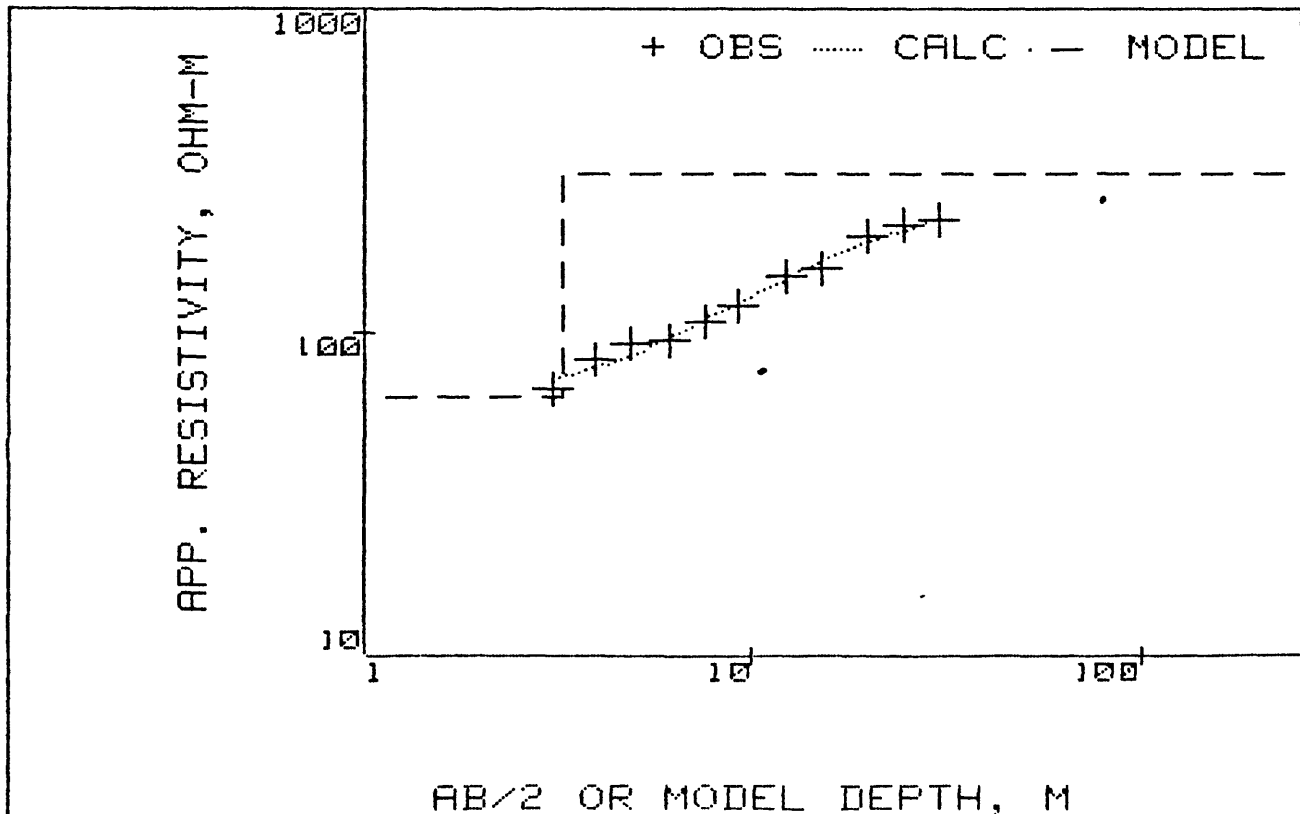
COORDINATES: 0 0
ELEVATION : 0
AZIMUTH :

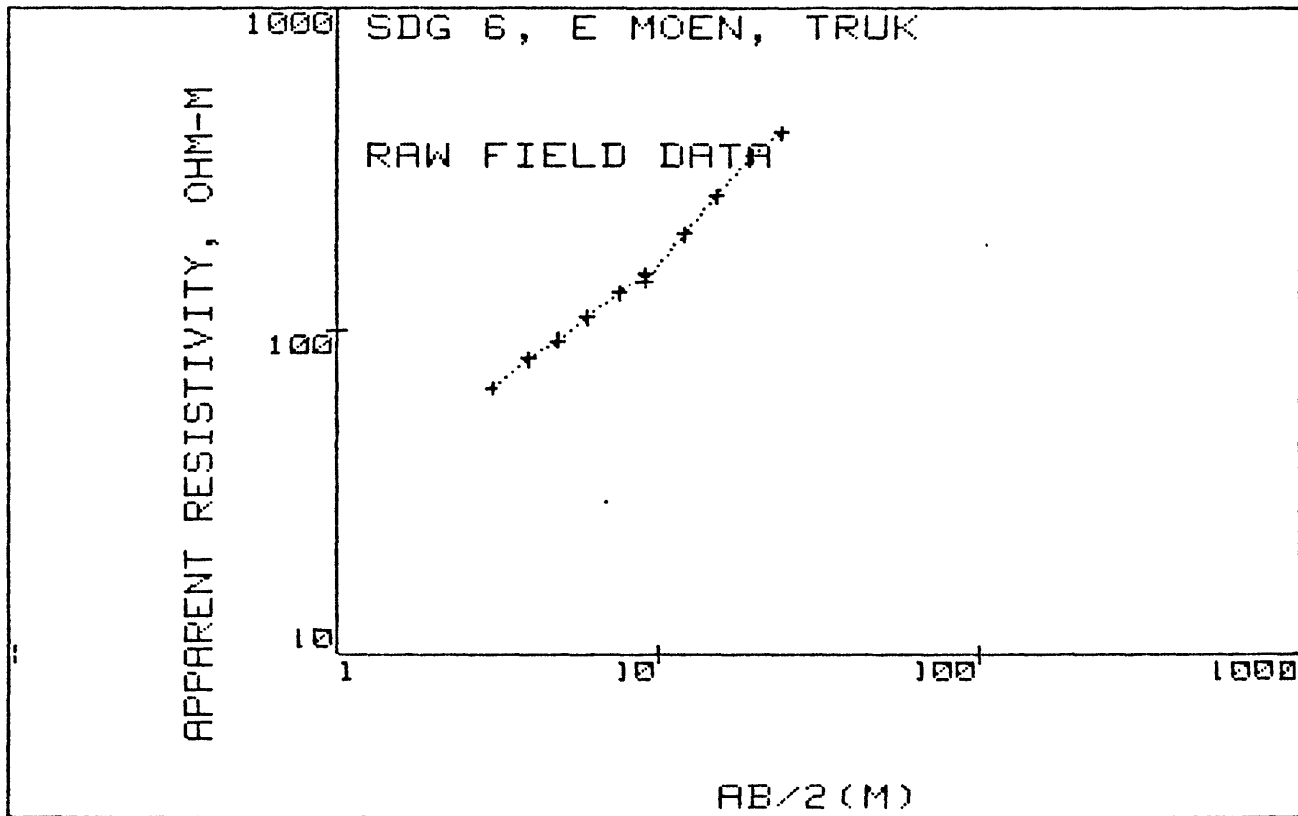
B-SD	B	B+SD
5.887E+001	6.309E+001	6.761E+001
2.841E+002	3.096E+002	3.374E+002
2.865E+000	3.255E+000	3.698E+000

FINAL UNSCALED PARAMETERS--
(* denotes fixed value)

	RESISTIVITY	DEPTH
1	6.30890707E+01	1 6.308907E+01
2	3.09610317E+02	2 3.096103E+02
3	3.25481876E+00	1 3.254819E+00

SDG 5,E MOEN, TRUK





AB/2 (M)	APP. RHO
3.0	66.1
4.0	81.6
4.9	92.6
6.1	108.8
7.6	129.3
9.1	148.0
9.1	141.0
12.2	197.5
15.2	257.6
19.8	345.1
24.4	410.0

MARQUARDT STATISTICS: SDG 6, E MDEN, TRUK

	X	OBSERVED	PREDICTED	%RESIDUALS	WEIGHT FN
1	+3.0480E+00	+6.2974E+01	+6.2767E+01	+3.2768E-01	+3.1114E+00
2	+3.9624E+00	+7.7741E+01	+7.5936E+01	+2.3214E+00	+2.0417E+00
3	+4.8768E+00	+8.8220E+01	+9.0274E+01	-2.3278E+00	+1.5854E+00
4	+6.0960E+00	+1.0365E+02	+1.0975E+02	-5.8832E+00	+1.1484E+00
5	+7.6200E+00	+1.2318E+02	+1.3360E+02	-8.4525E+00	+8.1314E-01
6	+9.1440E+00	+1.4100E+02	+1.5651E+02	-1.1003E+01	+6.2064E-01
7	+1.2192E+01	+1.9750E+02	+1.9951E+02	-1.0181E+00	+3.1633E-01
8	+1.5240E+01	+2.5760E+02	+2.3909E+02	+7.1864E+00	+1.8595E-01
9	+1.9812E+01	+3.4510E+02	+2.9289E+02	+1.5128E+01	+1.0361E-01
10	+2.4384E+01	+4.1000E+02	+3.4099E+02	+1.6831E+01	+7.3402E-02

CORRELATION MATRIX:

	1	3
1	+1.00	+.99
3	+.99	+1.00

REDUCED CHI-SQUARED=114.7
 PHI=802.83

DCLAG: ***** END *****

SDG 6, E MOEN, TRUK

COORDINATES: 0 0

ELEVATION : 0

AZIMUTH :

B-SD	B	B+SD
3.270E+001	4.438E+001	6.023E+001
	1.000E+003	
1.609E+000	2.236E+000	3.107E+000

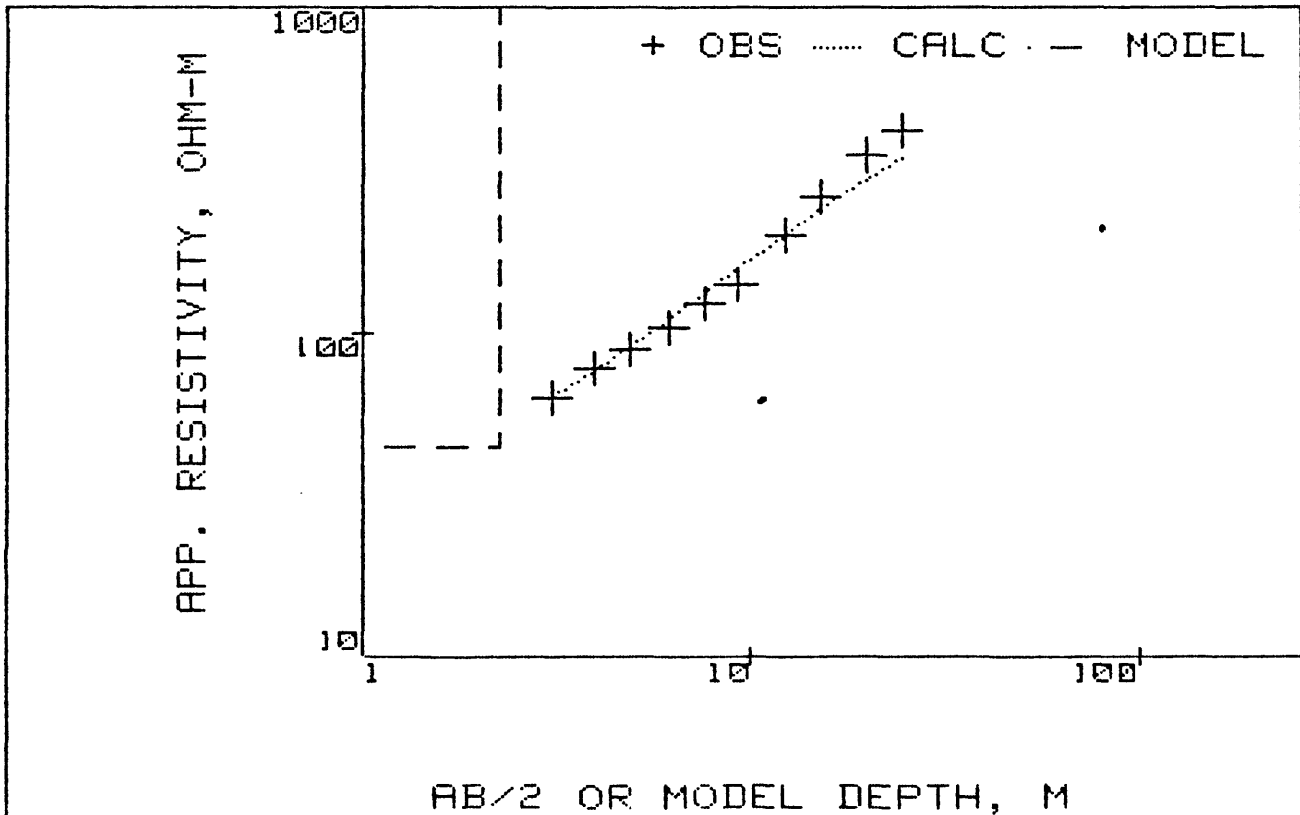
FINAL UNSCALED PARAMETERS--
(* denotes fixed value)

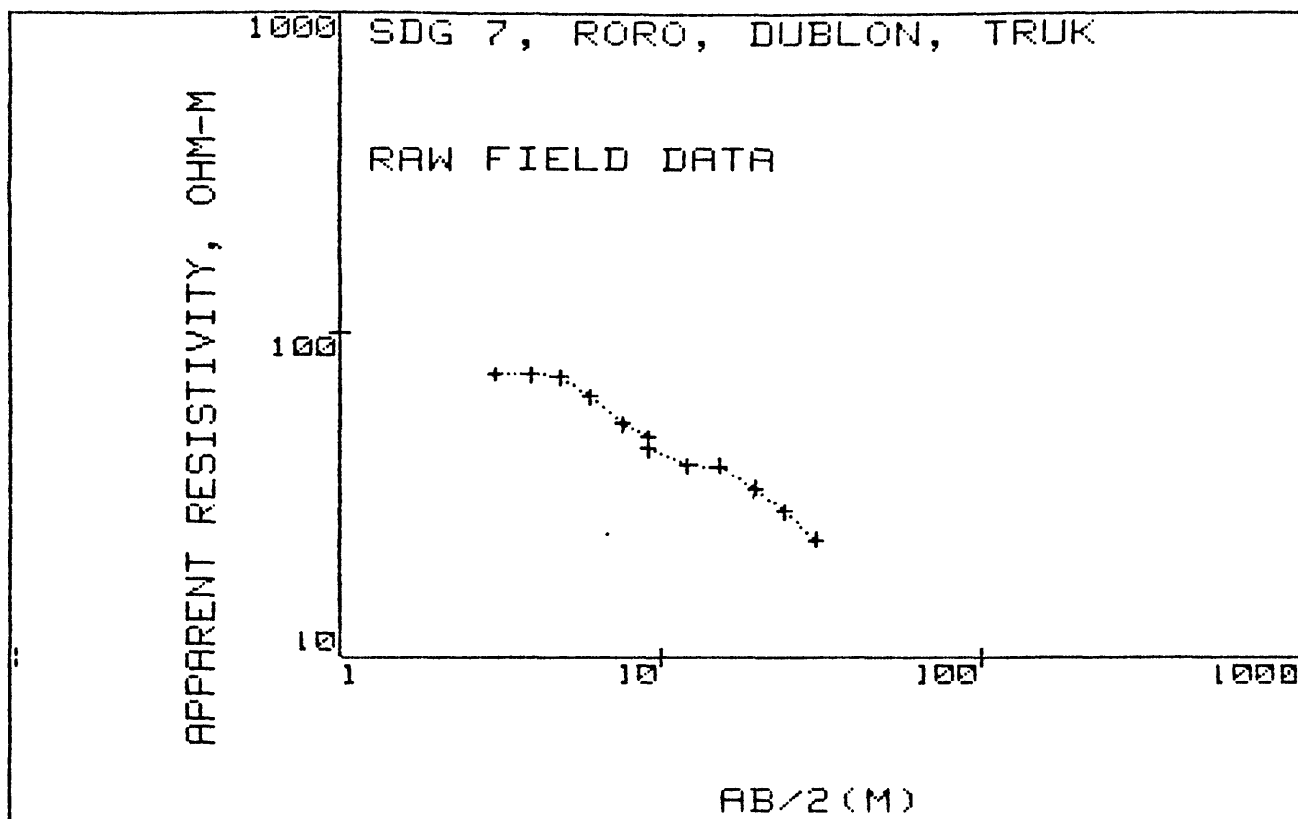
RESISTIVITY

DEPTH

1	4.43807168E+01	1	4.438072E+01	
2	* 1.00000000E+03	2	1.000000E+03	
3	2.23564011E+00			1 2.235640E+00

SDG 6, E MOEN, TRUK





AB/2 (M) APP. RHO

3.0	74.2
4.0	73.7
4.9	72.4
6.1	63.5
7.6	52.4
9.1	47.3
9.1	44.0
12.2	39.3
15.2	38.8
19.8	33.4
24.4	28.3
30.5	23.1

MARQUARDT STATISTICS: SDG 7, RORO, DUBLON, TRUK

	X	OBSERVED	PREDICTED	%RESIDUALS	WEIGHT FN
1	+3.0480E+00	+6.9023E+01	+7.2477E+01	-5.0044E+00	+3.2077E-01
2	+3.9624E+00	+6.8558E+01	+6.7739E+01	+1.1947E+00	+3.2514E-01
3	+4.8768E+00	+6.7349E+01	+6.2774E+01	+6.7932E+00	+3.3692E-01
4	+6.0960E+00	+5.9070E+01	+5.6689E+01	+4.0299E+00	+4.3798E-01
5	+7.6200E+00	+4.8744E+01	+5.0602E+01	-3.8109E+00	+6.4319E-01
6	+9.1440E+00	+4.4000E+01	+4.6161E+01	-4.9105E+00	+7.8937E-01
7	+1.2192E+01	+3.9300E+01	+4.0600E+01	-3.3089E+00	+9.8947E-01
8	+1.5240E+01	+3.8800E+01	+3.7254E+01	+3.9833E+00	+1.0151E+00
9	+1.9812E+01	+3.3400E+01	+3.3513E+01	-3.3963E-01	+1.3699E+00
10	+2.4384E+01	+2.8300E+01	+3.0019E+01	-6.0758E+00	+1.9082E+00
11	+3.0480E+01	+2.3100E+01	+2.5283E+01	-9.4500E+00	+2.8639E+00

CORRELATION MATRIX:

	1	2	3	4	5
1	+1.00	+.65	+.46	-.85	-.48
2	+.65	+1.00	+.85	-.92	-.89
3	+.46	+.85	+1.00	-.70	-1.00
4	-.85	-.92	-.70	+1.00	+.73
5	-.48	-.89	-1.00	+.73	+1.00

REDUCED CHI-SQUARED=56.13
 PHI=280.64

DCLAG: ***** END *****

SDG 7, RORO, DUBLON, TRUK

COORDINATES: 0 0

ELEVATION : 0

AZIMUTH :

B-SD	B	B+SD
5.987E+001	7.894E+001	1.041E+002
2.126E+001	3.611E+001	6.134E+001
0.000E+000	5.000E-002	1.000E+100
1.178E+000	2.727E+000	6.314E+000
8.357E-002	2.038E+001	4.968E+003

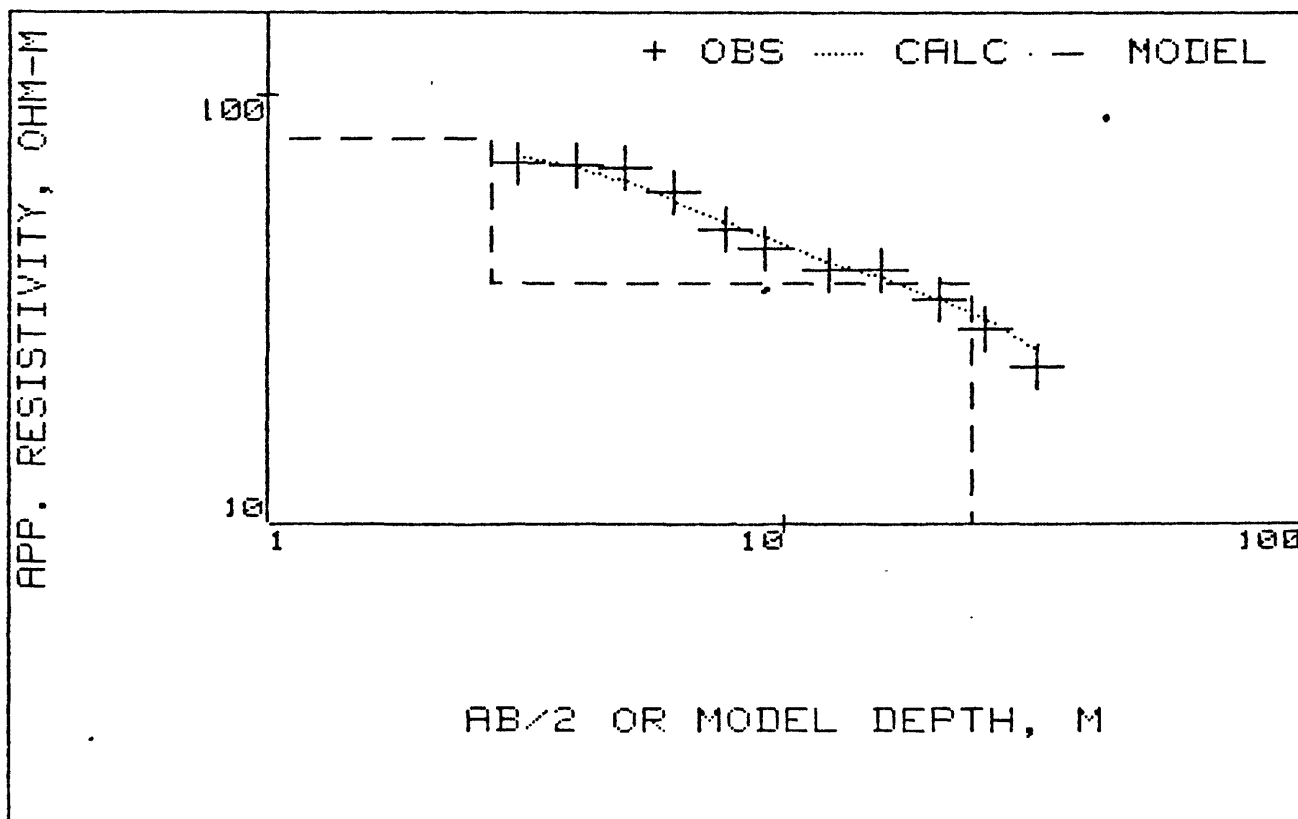
FINAL UNSCALED PARAMETERS--
(* denotes fixed value)

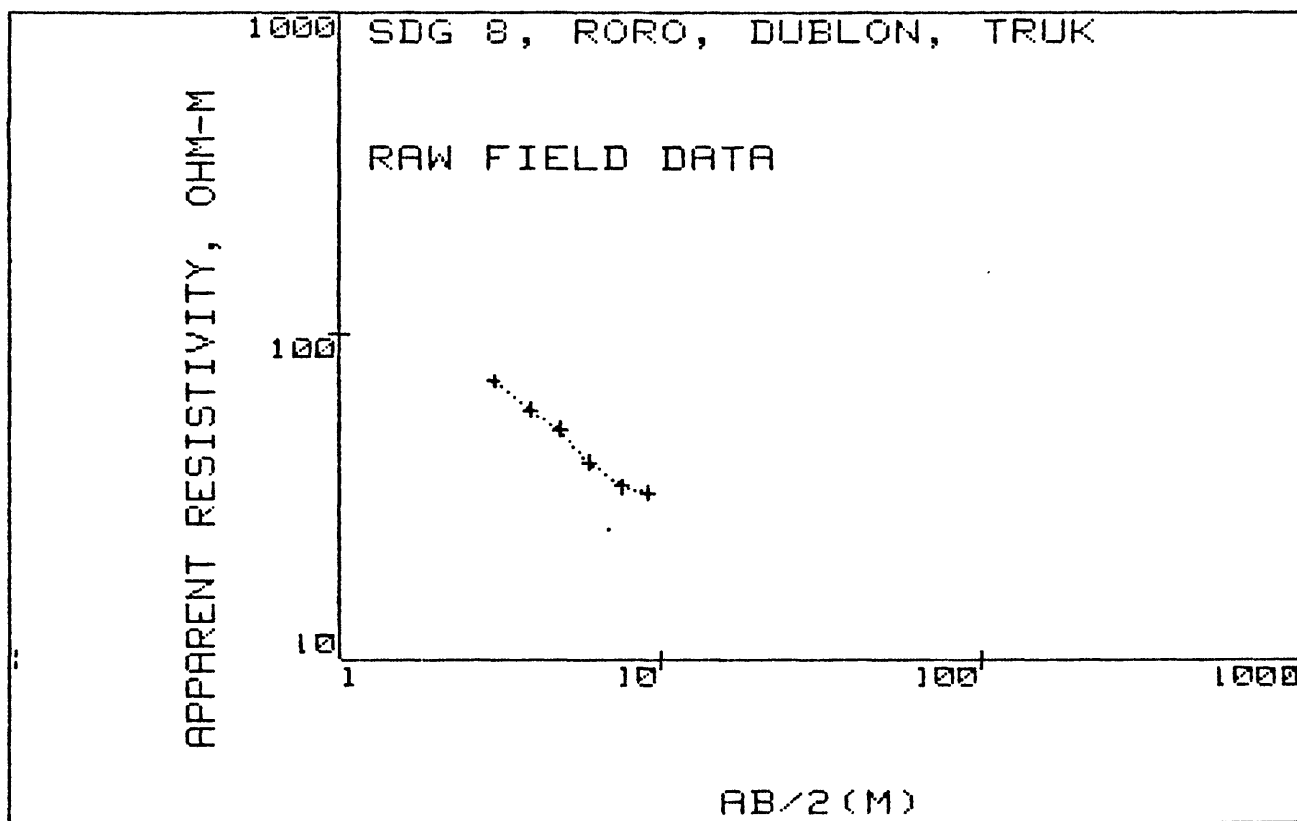
RESISTIVITY

DEPTH

1	7.89363615E+01	1	7.893636E+01		
2	3.61117899E+01	2	3.611179E+01		
3	5.00000000E-02	3	5.000000E-02		
4	2.72742512E+00			1	2.727425E+00
5	2.03760305E+01			2	2.310346E+01

SDG 7, RORO, DUBLON, TRUK





AB/2 (M)	APP. RHO
3.0	71.5
4.0	58.4
4.9	50.7
6.1	40.3
7.6	34.3
9.1	32.8

MARQUARDT STATISTICS: SDG 8, RORO, DUBLON, TRUK

	X	OBSERVED	PREDICTED	%RESIDUALS	WEIGHT FN
1	+3.0480E+00	+7.1500E+01	+7.1687E+01	-2.6145E-01	+3.5858E-01
2	+3.9624E+00	+5.8400E+01	+5.8907E+01	-8.6735E-01	+5.3749E-01
3	+4.8768E+00	+5.0700E+01	+4.9232E+01	+2.8961E+00	+7.1315E-01
4	+6.0960E+00	+4.0300E+01	+4.0802E+01	-1.2459E+00	+1.1287E+00
5	+7.6200E+00	+3.4300E+01	+3.5062E+01	-2.2220E+00	+1.5581E+00
6	+9.1440E+00	+3.2800E+01	+3.2179E+01	+1.8944E+00	+1.7039E+00

CORRELATION MATRIX:

	1	2	3
1	+1.00	+0.75	-0.93
2	+0.75	+1.00	-0.90
3	-0.93	-0.90	+1.00

REDUCED CHI-SQUARED=9.643
PHI=19.286

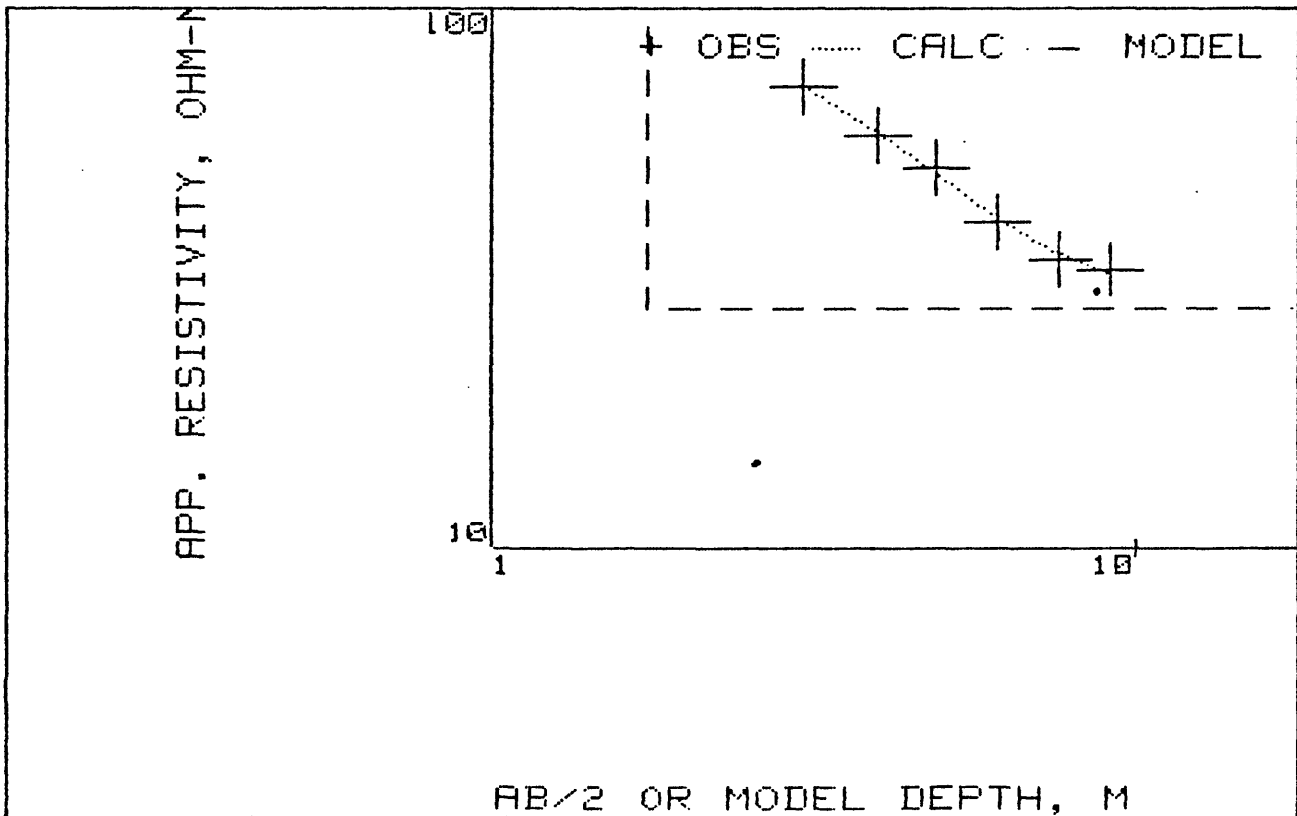
COORDINATES: 0 0
 ELEVATION : 0
 AZIMUTH :

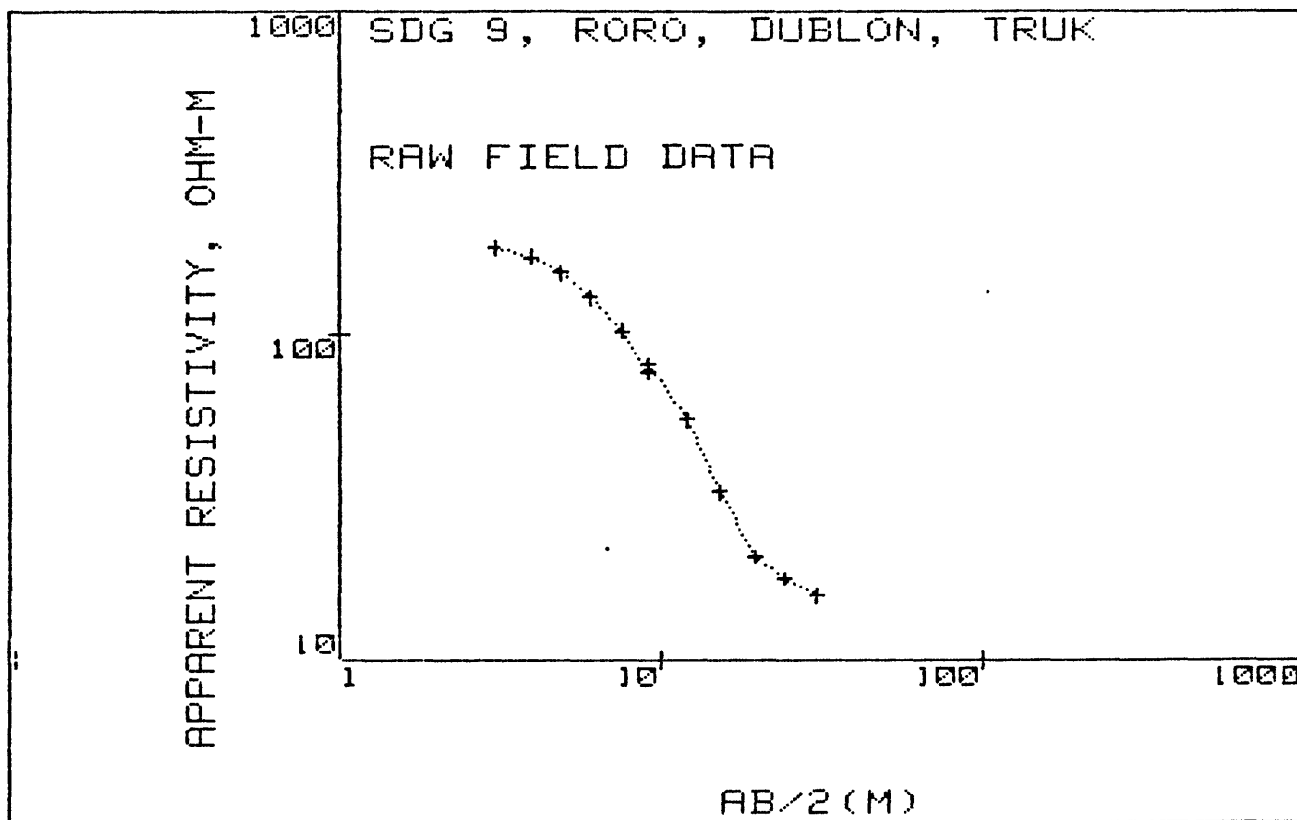
B-SD	B	B+SD
8.152E+001	1.007E+002	1.245E+002
2.451E+001	2.781E+001	3.155E+001
1.405E+000	1.744E+000	2.166E+000

FINAL UNSCALED PARAMETERS--
 (* denotes fixed value)

	RESISTIVITY	DEPTH
1	1.00733975E+02	1 1.007340E+02
2	2.78064330E+01	2 2.780643E+01
3	1.74410454E+00	1 1.744105E+00

SDG 8, RORO, DUBLON, TRUK





AB/2 (M)	APP. RHO
3.0	182.2
4.0	171.4
4.9	153.8
6.1	129.6
7.6	101.6
9.1	76.4
9.1	79.6
12.2	54.5
15.2	32.9
19.8	20.9
24.4	17.9
30.5	15.9

	X	OBSERVED	PREDICTED	%RESIDUALS	WEIGHT FN
1	+3.0480E+00	+1.8983E+02	+1.8611E+02	+1.9591E+00	+2.7684E-02
2	+3.9624E+00	+1.7858E+02	+1.7416E+02	+2.4772E+00	+3.1282E-02
3	+4.8768E+00	+1.6024E+02	+1.5916E+02	+6.7348E-01	+3.8852E-02
4	+6.0960E+00	+1.3503E+02	+1.3677E+02	-1.2883E+00	+5.4716E-02
5	+7.6200E+00	+1.0586E+02	+1.0896E+02	-2.9295E+00	+8.9029E-02
6	+9.1440E+00	+7.9600E+01	+8.4674E+01	-6.3747E+00	+1.5745E-01
7	+1.2192E+01	+5.4500E+01	+5.0642E+01	+7.0794E+00	+3.3587E-01
8	+1.5240E+01	+3.2900E+01	+3.2510E+01	+1.1859E+00	+9.2166E-01
9	+1.9812E+01	+2.0900E+01	+2.1243E+01	-1.6407E+00	+2.2839E+00
10	+2.4384E+01	+1.7900E+01	+1.7613E+01	+1.6050E+00	+3.1135E+00
11	+3.0480E+01	+1.5900E+01	+1.6146E+01	-1.5441E+00	+3.9461E+00

CORRELATION MATRIX:

	1	2	3
1	+1.00	+0.34	-0.74
2	+0.34	+1.00	-0.63
3	-0.74	-0.63	+1.00

REDUCED CHI-SQUARED=17.21

PHI=120.48

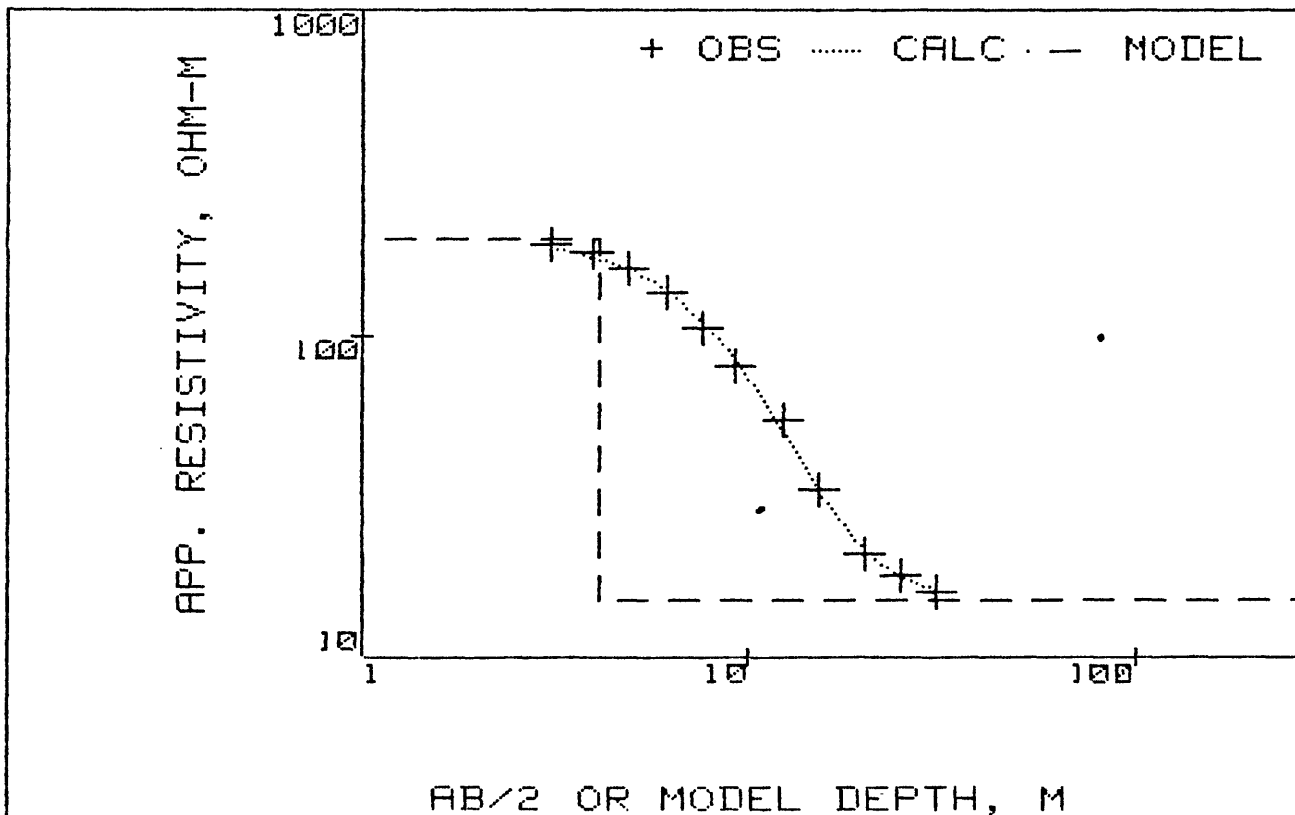
COORDINATES: 0 0
 ELEVATION : 0
 AZIMUTH :

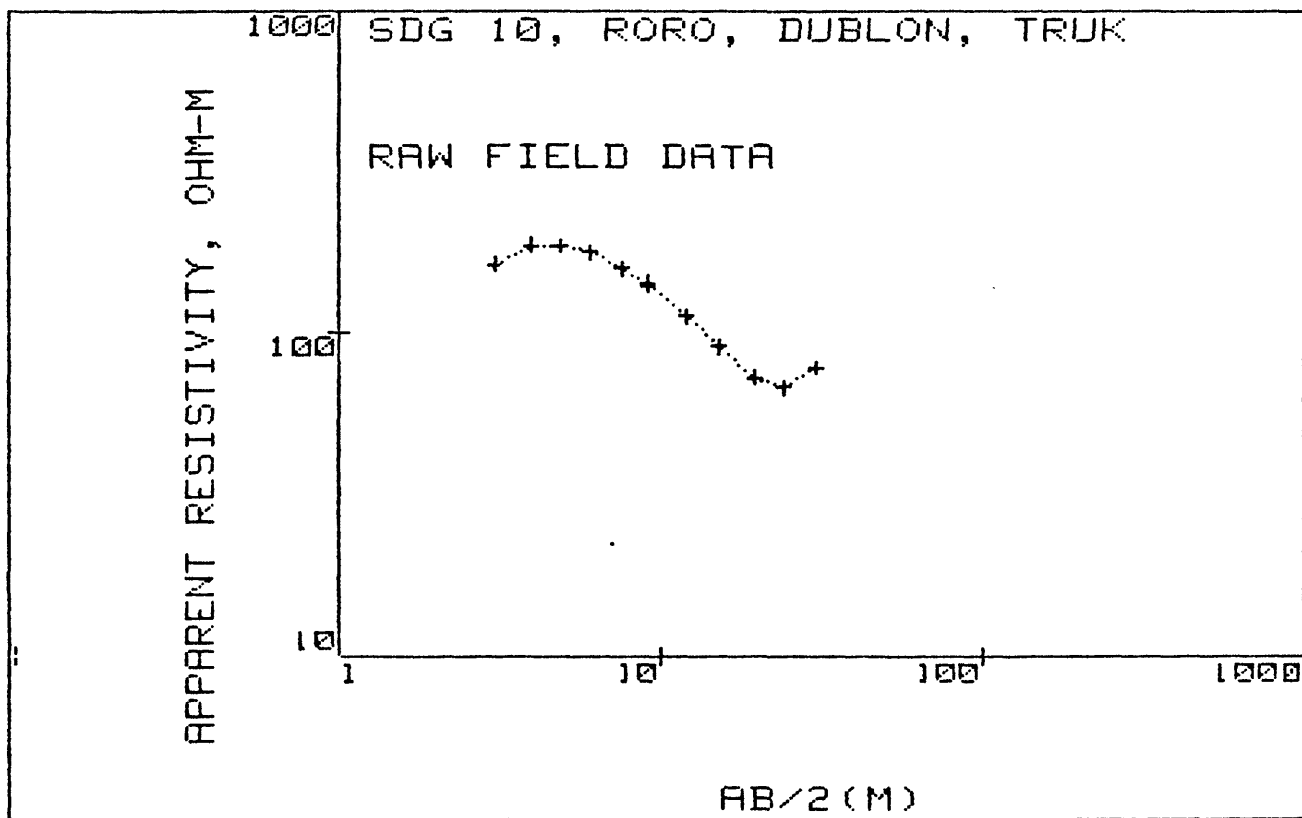
B-SD	B	B+SD
1.832E+002	1.990E+002	2.161E+002
1.354E+001	1.497E+001	1.656E+001
3.865E+000	4.123E+000	4.397E+000

FINAL UNSCALED PARAMETERS--
 (* denotes fixed value)

	RESISTIVITY	DEPTH
1	1.98953874E+02	1 1.989539E+02
2	1.49714993E+01	2 1.497150E+01
3	4.12265677E+00	1 4.122657E+00

SDG 9, RORO, DUBLON, TRUK





AB/2 (M)	APP. RHO
3.0	161.9
4.0	184.9
4.9	184.0
6.1	175.6
7.6	156.6
9.1	138.7
9.1	141.6
12.2	110.9
15.2	89.8
19.8	71.7
24.4	67.3
30.5	77.4

MARQUARDT STATISTICS: SDG 10, RORO, DUBLON, TRUK

	X	OBSERVED	PREDICTED	%RESIDUALS	WEIGHT FN
1	+3.0480E+00	+1.6529E+02	+1.6846E+02	-1.9193E+00	+4.0238E-01
2	+3.9624E+00	+1.8877E+02	+1.8228E+02	+3.4345E+00	+3.0850E-01
3	+4.8768E+00	+1.8785E+02	+1.8570E+02	+1.1423E+00	+3.1153E-01
4	+6.0960E+00	+1.7927E+02	+1.7978E+02	-2.8240E-01	+3.4204E-01
5	+7.6200E+00	+1.5987E+02	+1.6360E+02	-2.3332E+00	+4.3008E-01
6	+9.1440E+00	+1.4160E+02	+1.4434E+02	-1.9359E+00	+5.4825E-01
7	+1.2192E+01	+1.1090E+02	+1.0993E+02	+8.7716E-01	+8.9380E-01
8	+1.5240E+01	+8.9800E+01	+8.7184E+01	+2.9130E+00	+1.3632E+00
9	+1.9812E+01	+7.1700E+01	+7.1781E+01	-1.1244E-01	+2.1383E+00
10	+2.4384E+01	+6.7300E+01	+6.9569E+01	-3.3718E+00	+2.4270E+00
11	+3.0480E+01	+7.7400E+01	+7.5753E+01	+2.1283E+00	+1.8349E+00

CORRELATION MATRIX:

	1	2	3	5	6	7
1	+1.00	+.99	-.45	+1.00	-.99	+.55
2	+.99	+1.00	-.33	+.99	-1.00	+.66
3	-.45	-.33	+1.00	-.44	+.34	+.49
5	+1.00	+.99	-.44	+1.00	-.99	+.56
6	-.99	-1.00	+.34	-.99	+1.00	-.65
7	+.55	+.66	+.49	+.56	-.65	+1.00

REDUCED CHI-SQUARED=12.81
 PHI=51.222

DCLAG: ***** END *****

SDG 10, RORD, DUBLON, TRUK

COORDINATES: 0 0
ELEVATION : 0
AZIMUTH :

B-SD	B	B+SD
7.183E-060	6.731E+001	6.307E+062
5.054E-058	7.297E+002	1.053E+063
2.826E+001	4.196E+001	6.232E+001
	1.000E+003	
5.589E-071	7.609E-001	1.036E+070
1.142E-066	1.154E+000	1.165E+066
8.721E+000	1.644E+001	3.098E+001

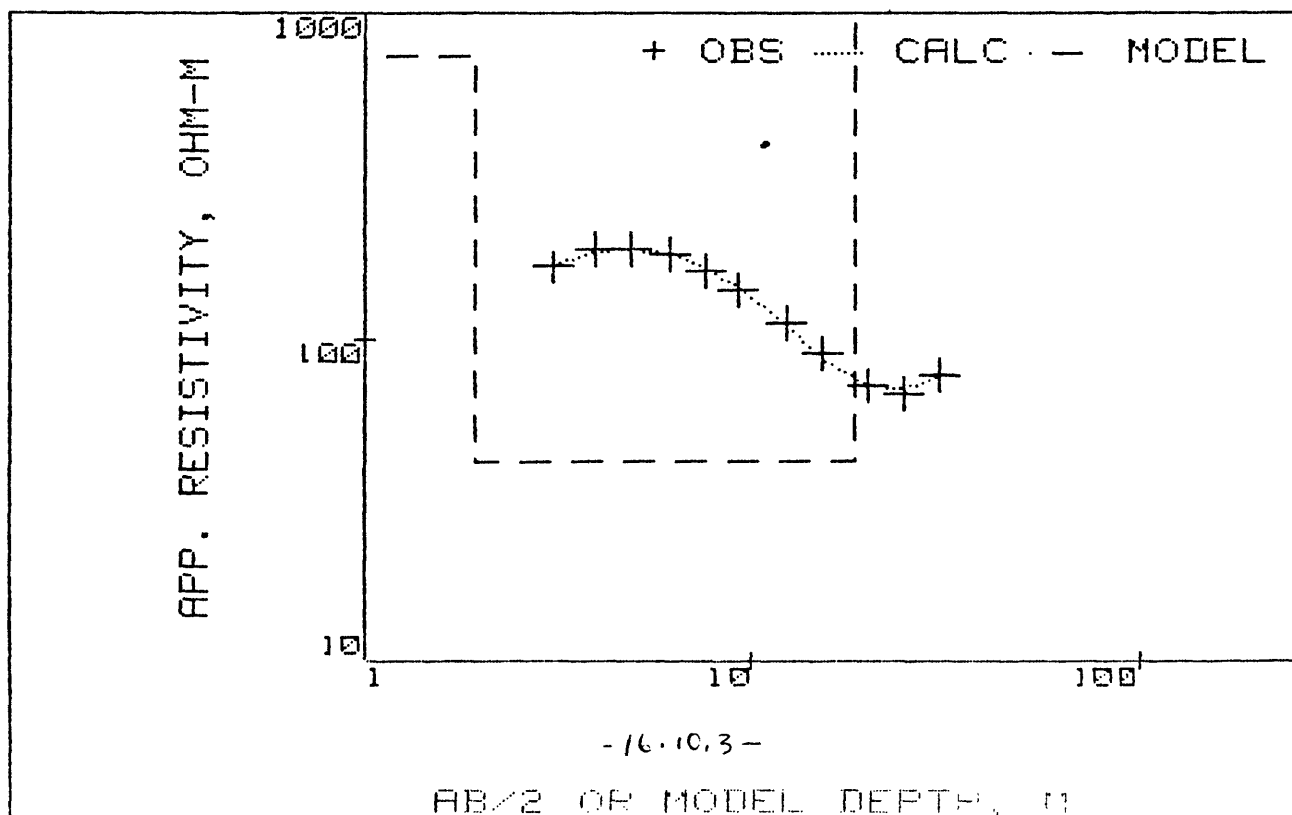
FINAL UNSCALED PARAMETERS--
(* denotes fixed value)

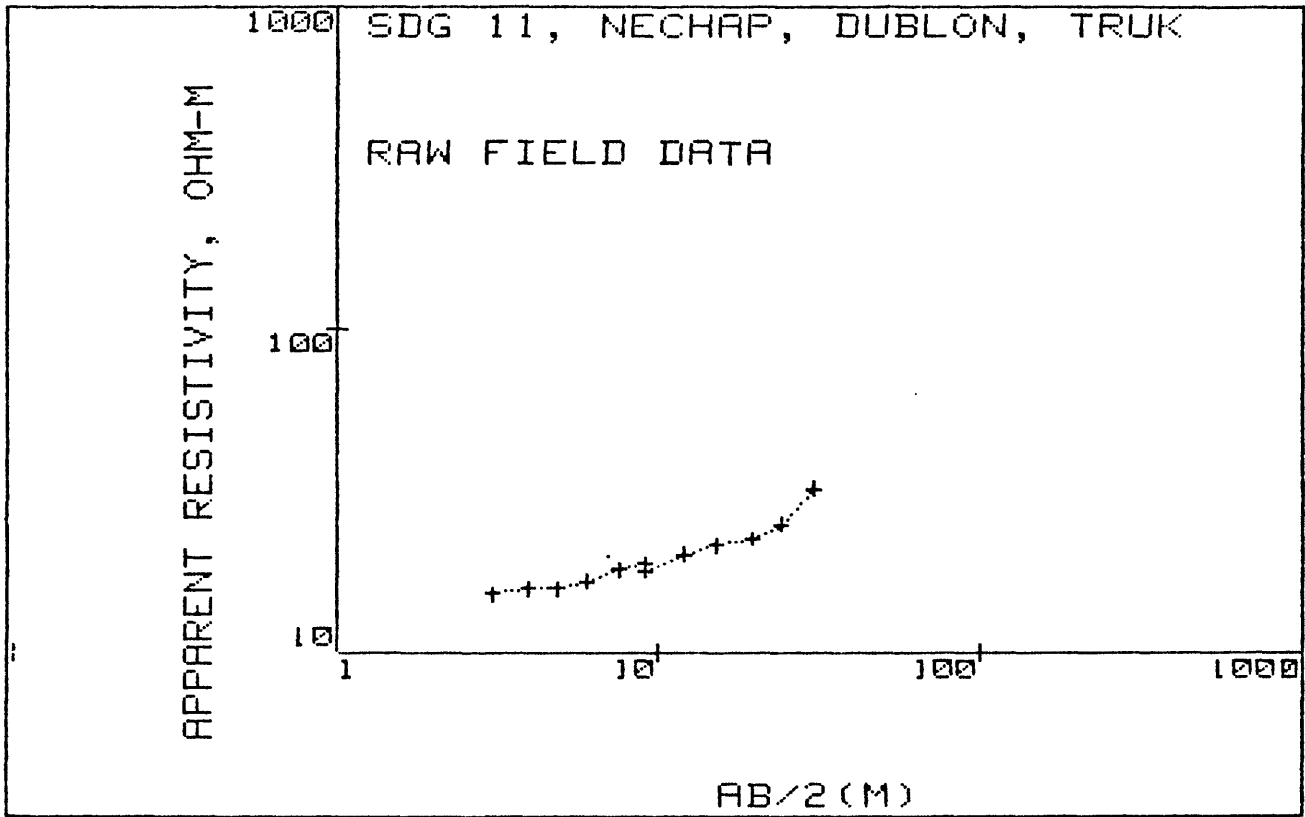
RESISTIVITY

DEPTH

1	6.73097753E+01	1	6.730978E+01		
2	7.29679451E+02	2	7.296795E+02		
3	4.19611120E+01	3	4.196111E+01		
4 *	1.00000000E+03	4	1.000000E+03		
5	7.60929901E-01			1	7.609299E-01
6	1.15362235E+00			2	1.914552E+00
7	1.64370912E+01			3	1.835164E+01

SDG 10, RORD, DUBLON, TRUK





AB/2 (M)	APP. RHO
3.0	15.2
4.0	15.8
4.9	15.8
6.1	16.7
7.6	18.1
9.1	18.9
9.1	18.0
12.2	20.2
15.2	21.6
19.8	22.5
24.4	25.0
30.5	32.0

MARQUARDT STATISTICS: SDG 11, NECHAP, DUBLON, TRUK

	X	OBSERVED	PREDICTED	%RESIDUALS	WEIGHT FN
1	+3.0480E+00	+1.4476E+01	+1.4371E+01	+7.2501E-01	+1.5832E+00
2	+3.9624E+00	+1.5048E+01	+1.4853E+01	+1.2919E+00	+1.4652E+00
3	+4.8768E+00	+1.5048E+01	+1.5409E+01	-2.4028E+00	+1.4652E+00
4	+6.0960E+00	+1.5905E+01	+1.6183E+01	-1.7463E+00	+1.3115E+00
5	+7.6200E+00	+1.7238E+01	+1.7113E+01	+7.2517E-01	+1.1165E+00
6	+9.1440E+00	+1.8000E+01	+1.7970E+01	+1.6572E-01	+1.0240E+00
7	+1.2192E+01	+2.0200E+01	+1.9521E+01	+3.3631E+00	+8.1308E-01
8	+1.5240E+01	+2.1600E+01	+2.1012E+01	+2.7227E+00	+7.1110E-01
9	+1.9812E+01	+2.2500E+01	+2.3420E+01	-4.0902E+00	+6.5535E-01
10	+2.4384E+01	+2.5000E+01	+2.6183E+01	-4.7338E+00	+5.3083E-01
11	+3.0480E+01	+3.2000E+01	+3.0422E+01	+4.9326E+00	+3.2399E-01

CORRELATION MATRIX:

	1	2	4	5
1	+1.00	+.62	+.87	+.27
2	+.62	+1.00	+.90	+.84
4	+.87	+.90	+1.00	+.57
5	+.27	+.84	+.57	+1.00

REDUCED CHI-SQUARED=15.63
PHI=93.764

DCLAG: ***** END *****

SDG 11, NECHAP, DUBLON, TRUK

COORDINATES: 0 0

ELEVATION : 0

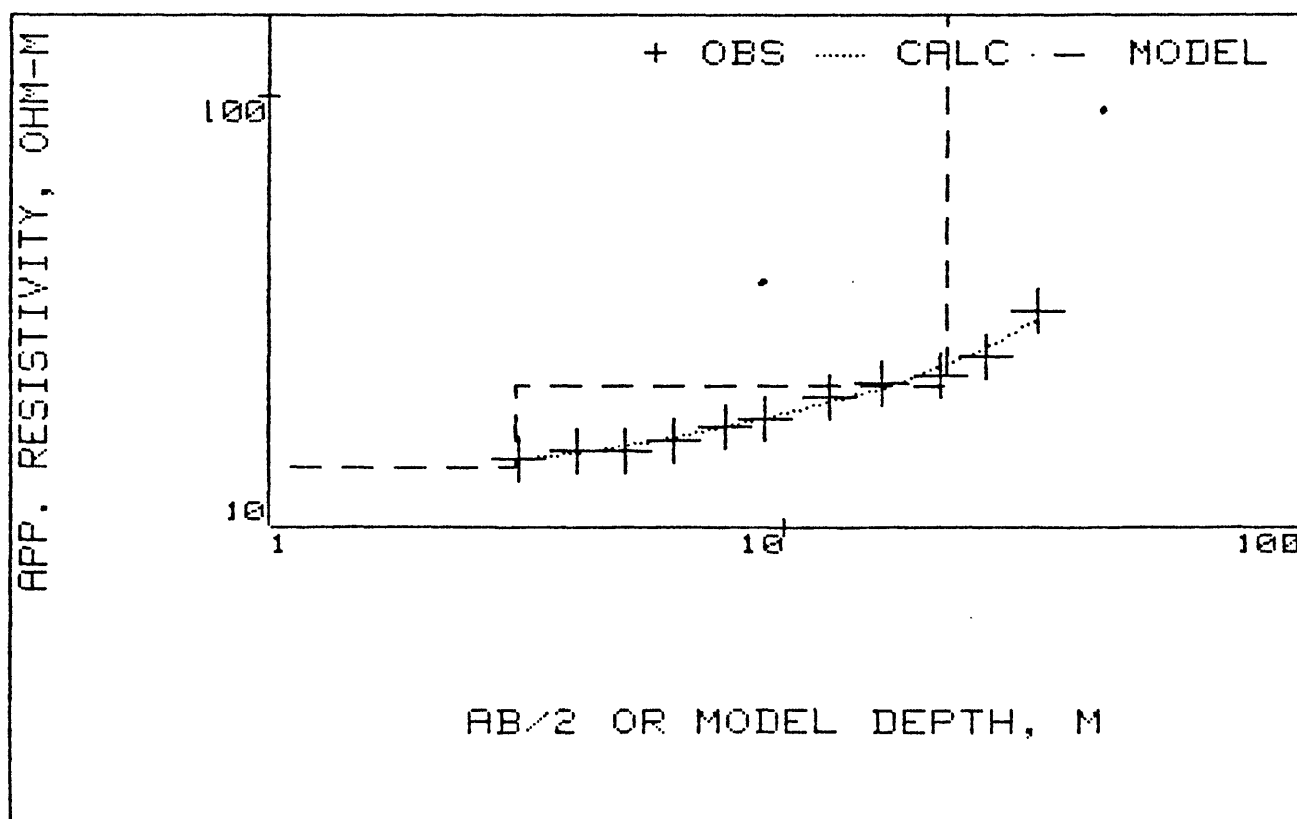
AZIMUTH :

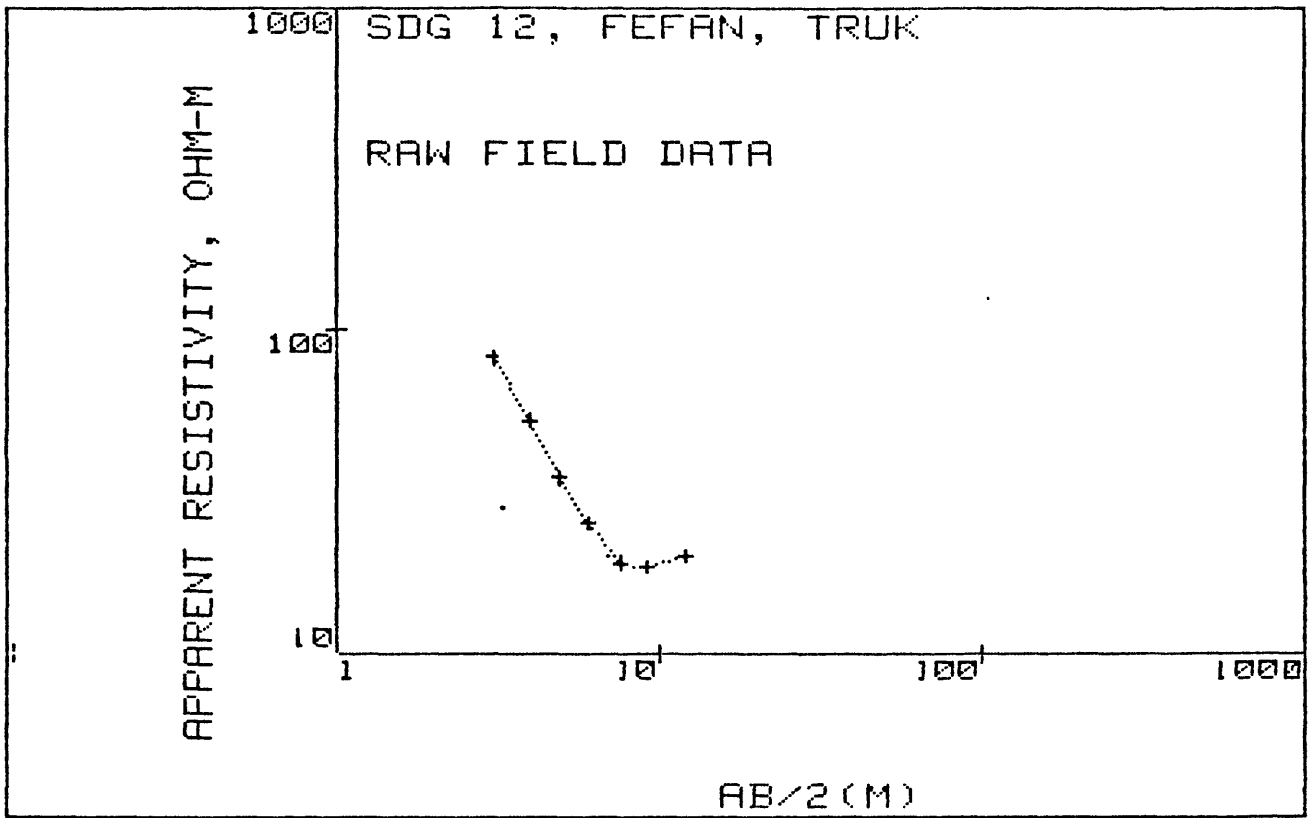
R-SD	B	B+SD
9.639E+000	1.378E+001	1.971E+001
1.013E+001	2.128E+001	4.472E+001
	1.000E+003	
2.882E-001	2.993E+000	3.108E+001
8.167E+000	1.750E+001	3.750E+001

FINAL UNSCALED PARAMETERS--
(* denotes fixed value)

	RESISTIVITY	DEPTH
1	1.37835427E+01	1 1.378354E+01
2	2.12829106E+01	2 2.128291E+01
3 *	1.00000000E+03	3 1.000000E+03
4	2.99271030E+00	1 2.992710E+00
5	1.75008321E+01	2 2.049354E+01

SDG 11, NECHAP, DUBLON, TRUK





AB/2 (M)	APP. RHO
3.0	81.4
4.0	51.7
4.9	34.9
6.1	25.3
7.6	19.1
9.1	18.6
12.2	20.1

MARQUARDT STATISTICS: SDG 12, FEFAN, TRUK

	X	OBSERVED	PREDICTED	%RESIDUALS	WEIGHT FN
1	+3.0480E+00	+8.1400E+01	+8.0644E+01	+9.2849E-01	+9.5909E-02
2	+3.9624E+00	+5.1700E+01	+5.2283E+01	-1.1270E+00	+2.3775E-01
3	+4.8768E+00	+3.4900E+01	+3.5400E+01	-1.4322E+00	+5.2174E-01
4	+6.0960E+00	+2.5300E+01	+2.4370E+01	+3.6747E+00	+9.9281E-01
5	+7.6200E+00	+1.9100E+01	+1.9536E+01	-2.2845E+00	+1.7420E+00
6	+9.1440E+00	+1.8600E+01	+1.8557E+01	+2.2928E-01	+1.8369E+00
7	+1.2192E+01	+2.0100E+01	+2.0051E+01	+2.4283E-01	+1.5729E+00

CORRELATION MATRIX:

	1	2	4	5
1	+1.00	+.73	-.95	+.66
2	+.73	+1.00	-.88	+.96
4	-.95	-.88	+1.00	-.80
5	+.66	+.96	-.80	+1.00

REDUCED CHI-SQUARED=11.51

PHI=23.017

DCLAG: ***** END *****

SDG 12, FEFAN, TRUK

COORDINATES: 0 0

ELEVATION : 0

AZIMUTH :

B-SD	B	B+SD
1.138E+002	1.755E+002	2.706E+002
9.588E+000	1.420E+001	2.104E+001
	4.000E+002	
1.146E+000	1.433E+000	1.794E+000
4.272E+000	9.406E+000	2.071E+001

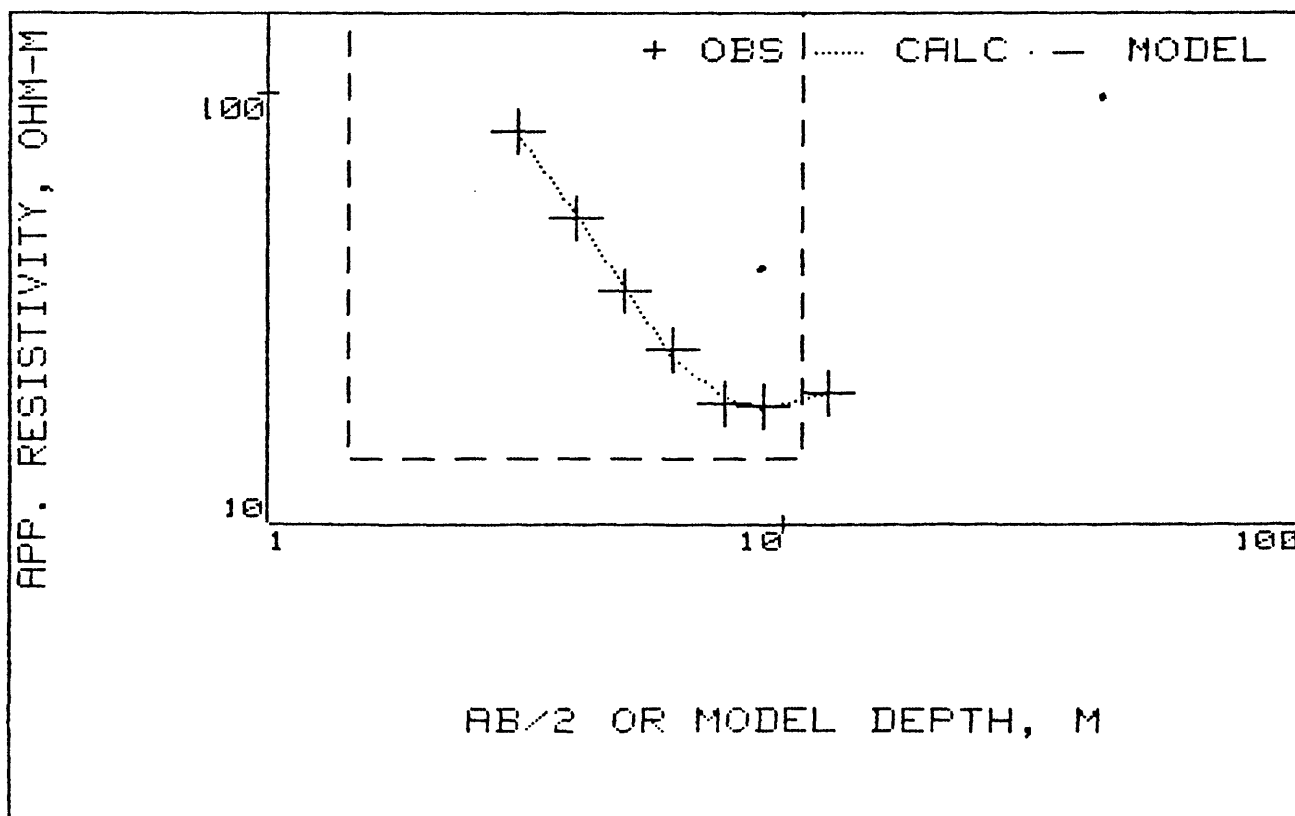
FINAL UNSCALED PARAMETERS--
(* denotes fixed value)

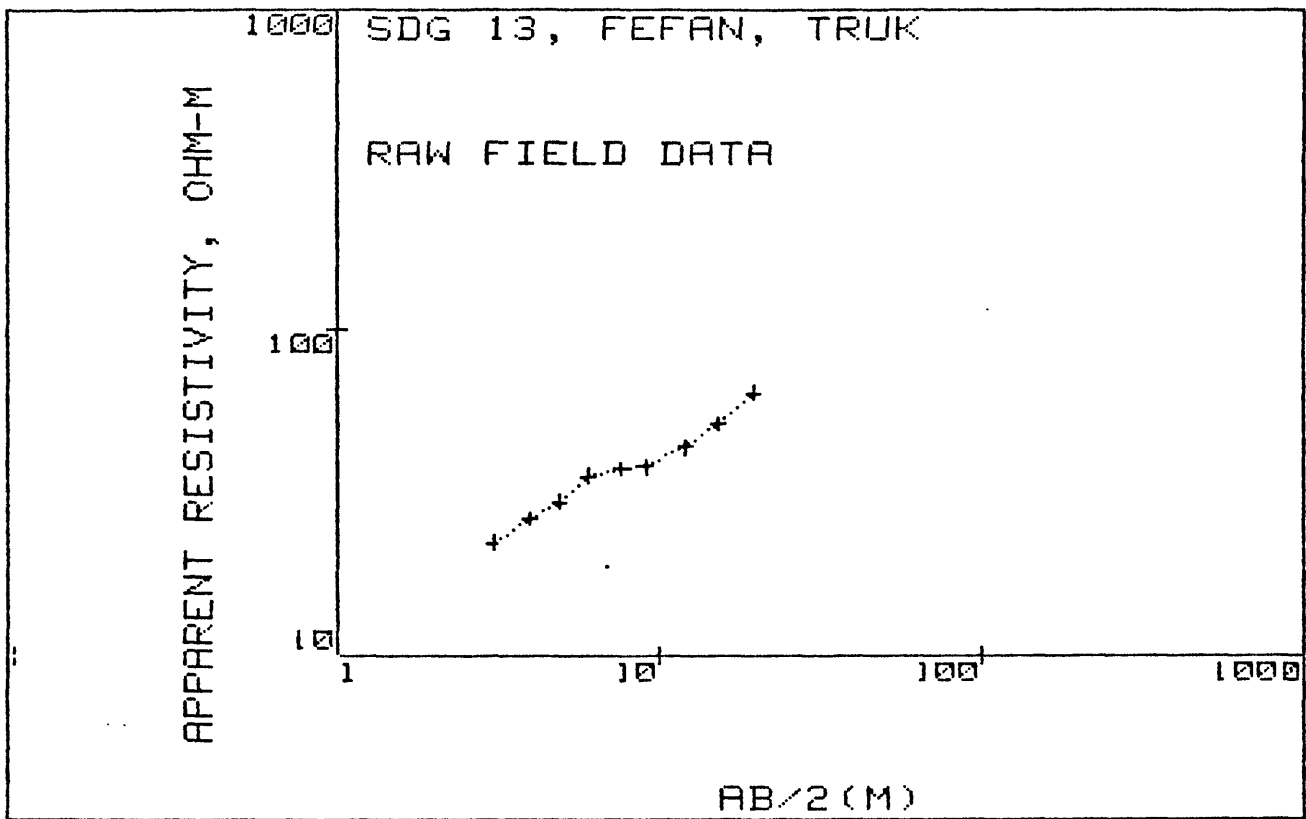
RESISTIVITY

DEPTH

1	1.75527064E+02	1	1.755271E+02		
2	1.42028096E+01	2	1.420281E+01		
3	* 4.00000000E+02	3	4.000000E+02		
4	1.43335519E+00			1	1.433355E+00
5	9.40578753E+00			2	1.083914E+01

SDG 12, FEFAN, TRUK





AB/2 (M)	APP. RHO
3.0	22.3
4.0	26.3
4.9	29.7
6.1	35.2
7.6	37.1
9.1	37.8
12.2	43.0
15.2	50.5
19.8	62.9

MARQUARDT STATISTICS: SDG 13, FEFAN, TRUK

	X	OBSERVED	PREDICTED	%RESIDUALS	WEIGHT FN
1	+3.0480E+00	+2.2300E+01	+2.3011E+01	-3.1896E+00	+2.2596E+00
2	+3.9624E+00	+2.6300E+01	+2.5729E+01	+2.1698E+00	+1.6245E+00
3	+4.8768E+00	+2.9700E+01	+2.8657E+01	+3.5133E+00	+1.2739E+00
4	+6.0960E+00	+3.5200E+01	+3.2485E+01	+7.7128E+00	+9.0689E-01
5	+7.6200E+00	+3.7100E+01	+3.6833E+01	+7.1894E-01	+8.1638E-01
6	+9.1440E+00	+3.7800E+01	+4.0618E+01	-7.4546E+00	+7.8642E-01
7	+1.2192E+01	+4.3000E+01	+4.6731E+01	-8.6756E+00	+6.0772E-01
8	+1.5240E+01	+5.0500E+01	+5.1376E+01	-1.7356E+00	+4.4061E-01
9	+1.9812E+01	+6.2900E+01	+5.6493E+01	+1.0185E+01	+2.8401E-01

CORRELATION MATRIX:

	1	2	3
1	+1.00	+0.58	+0.95
2	+0.58	+1.00	+0.78
3	+0.95	+0.78	+1.00

REDUCED CHI-SQUARED=64.96
 PHI=324.82

DCLAG: ***** END *****

SDG 13, FEFAN, TRUK

COORDINATES: 0 0

ELEVATION : 0

AZIMUTH :

B-SD	B	B+SD
1.086E+001	1.930E+001	3.430E+001
4.518E+001	7.463E+001	1.233E+002
8.682E-001	2.474E+000	7.050E+000

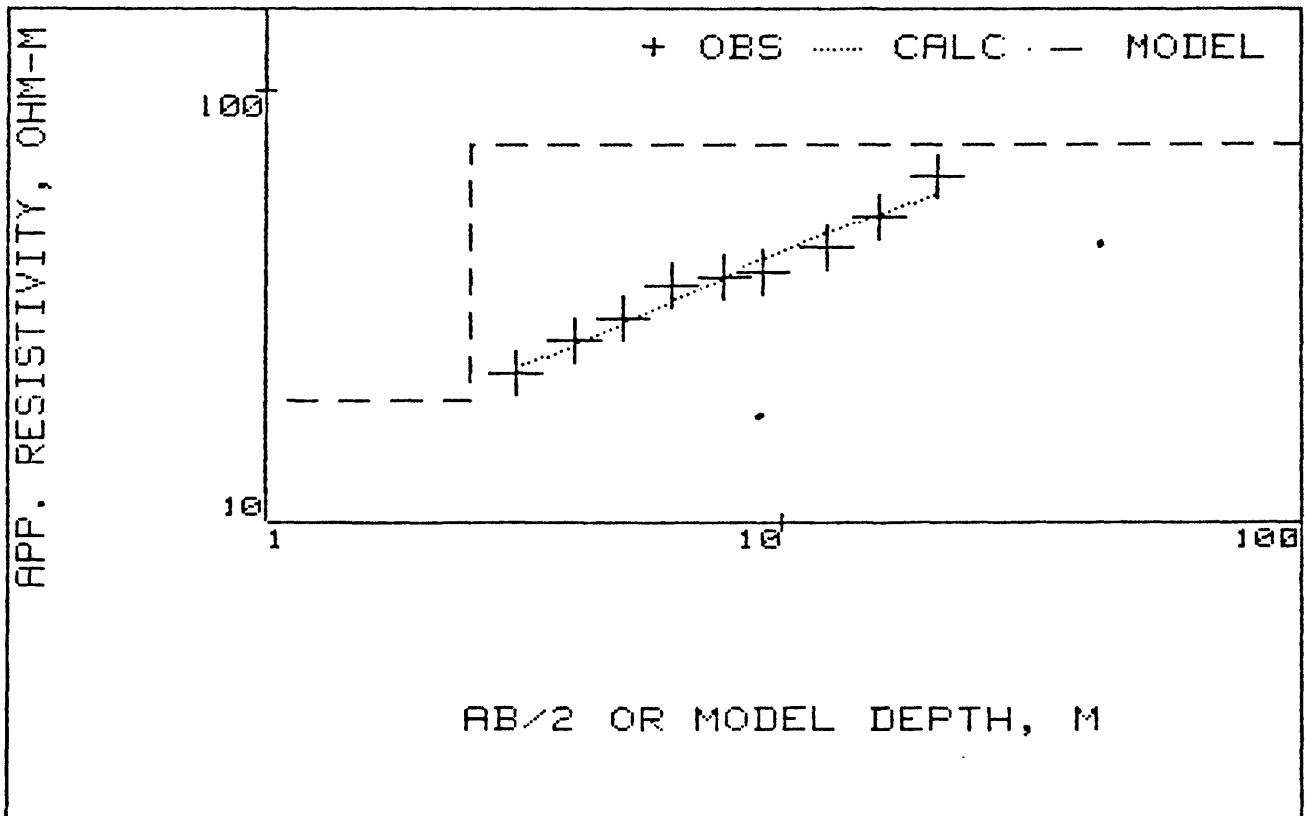
FINAL UNSCALED PARAMETERS--
(* denotes fixed value)

RESISTIVITY

DEPTH

1	1.93011832E+01	1	1.930118E+01	
2	7.46260827E+01	2	7.462608E+01	
3	2.47402870E+00			1 2.474029E+00

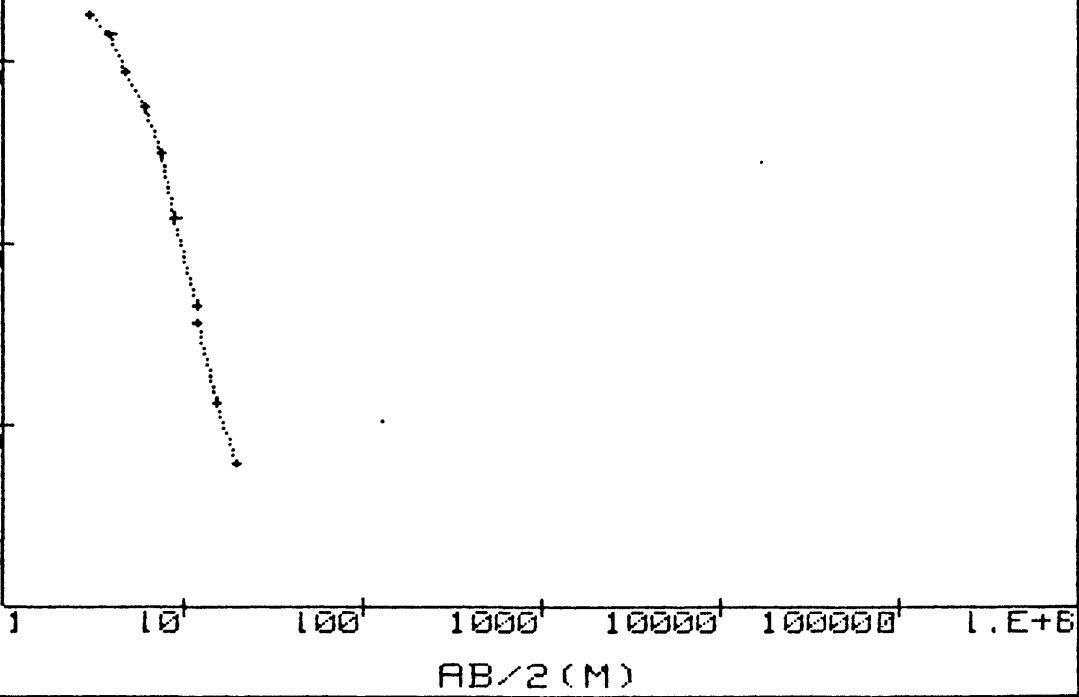
SDG 13, FEFAN, TRUK



10000 SDG 14, PIS, TRUK

APPARENT RESISTIVITY, OHM-M

RAW FIELD DATA



AB/2 (M)	APP. RHO
3.0	1832.0
4.0	1442.0
4.9	887.0
6.1	556.0
7.6	308.0
9.1	137.0
12.2	45.4
12.2	36.6
15.2	13.4
19.8	6.2

	X	OBSERVED	PREDICTED	%RESIDUALS	WEIGHT FN
1	+3.0480E+00	+1.4769E+03	+1.5010E+03	-1.6318E+00	+1.2721E-04
2	+3.9624E+00	+1.1625E+03	+1.0913E+03	+6.1224E+00	+2.0532E-04
3	+4.8768E+00	+7.1507E+02	+7.5732E+02	-5.9090E+00	+5.4264E-04
4	+6.0960E+00	+4.4823E+02	+4.4814E+02	+2.0388E-02	+1.3810E-03
5	+7.6200E+00	+2.4830E+02	+2.2854E+02	+7.9573E+00	+4.5004E-03
6	+9.1440E+00	+1.1044E+02	+1.1809E+02	-6.9212E+00	+2.2747E-02
7	+1.2192E+01	+3.6600E+01	+3.5331E+01	+3.4659E+00	+2.0713E-01
8	+1.5240E+01	+1.3400E+01	+1.3583E+01	-1.3684E+00	+1.5452E+00
9	+1.9812E+01	+6.2000E+00	+6.1835E+00	+2.6687E-01	+7.2181E+00

CORRELATION MATRIX:

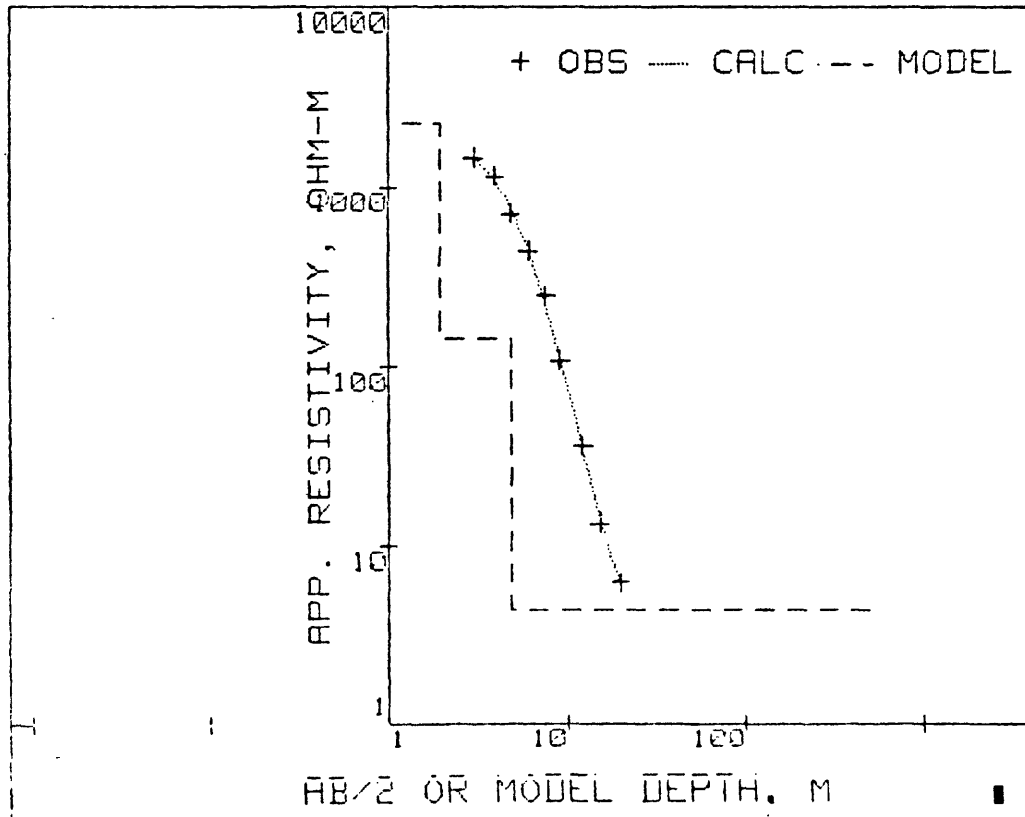
	1	2	3	4	5
1	+1.00	+.83	+.56	-.92	-.70
2	+.83	+1.00	+.82	-.97	-.97
3	+.56	+.82	+1.00	-.73	-.90
4	-.92	-.97	-.73	+1.00	+.89
5	-.70	-.97	-.90	+.89	+1.00

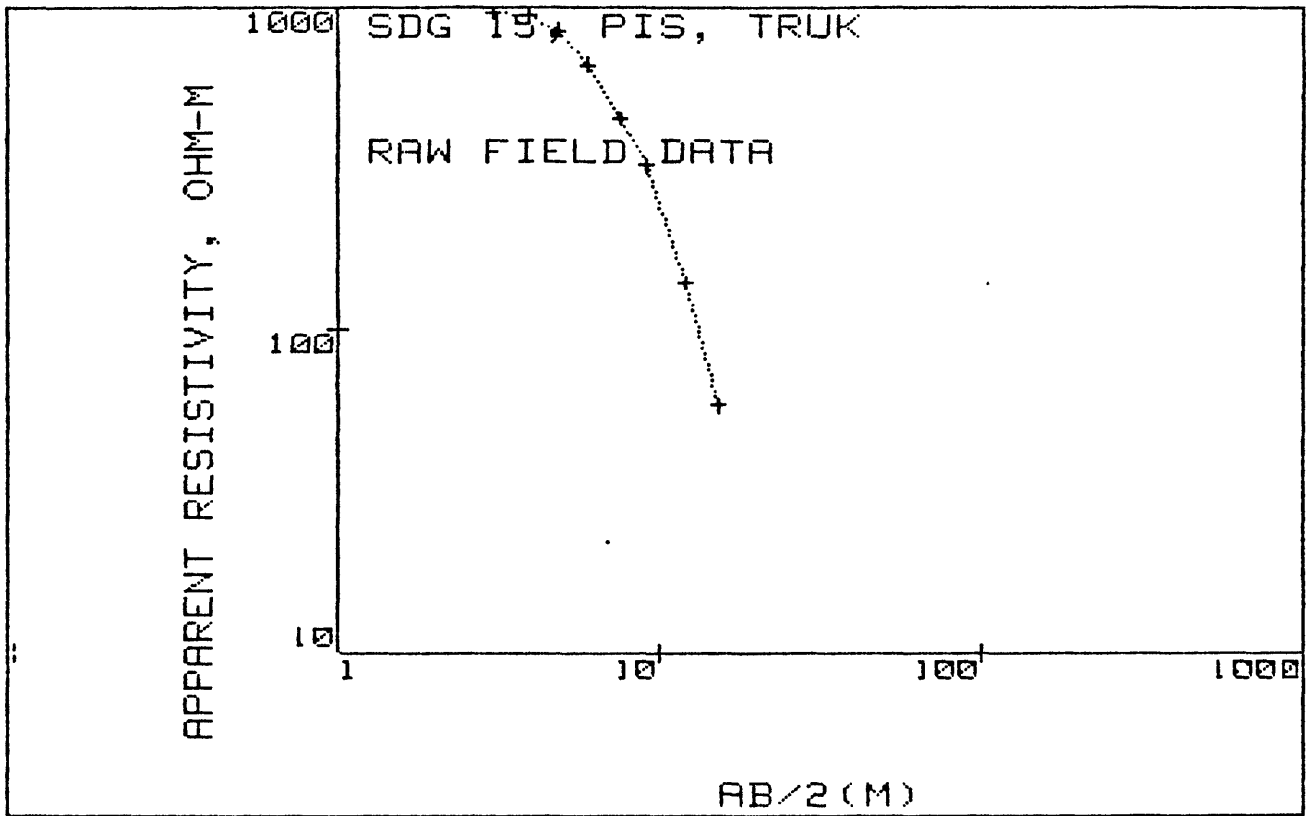
REDUCED CHI-SQUARED=66.75
 PHI=200.24

DCLAG: ***** END ***** SDG 14, PIS, TRUK
 COORDINATES: 0 0
 ELEVATION : 0
 AZIMUTH :

RESISTIVITY			THICKNESS			DEPTH	ELEV
859.0	2304.1	6180.3	.7	2.0	5.6	0.0	0.0
0.0	144.1	663787.6	.4	2.9	23.9	2.0	-2.0
.8	4.4	23.1				4.9	-4.9

SDG 14, PIS, TRUK





AB/2 (M)	APP. RHO
3.0	964.0
4.0	942.0
4.9	849.0
6.1	657.0
7.6	446.0
9.1	314.0
12.2	137.5
15.2	57.6

MARQUADT STATISTICS: SDG 15, PIS, TRUK

	X	OBSERVED	PREDICTED	%RESIDUALS	WEIGHT FN
1	+3.0490E+00	+9.6400E+02	+9.8623E+02	-2.3681E+00	+2.2933E-02
2	+3.9624E+00	+9.4200E+02	+9.3027E+02	+1.2450E+00	+2.4017E-02
3	+4.8756E+00	+8.4900E+02	+8.2135E+02	+3.2556E+00	+2.9567E-02
4	+6.0950E+00	+6.5700E+02	+6.5338E+02	+5.5128E-01	+4.9373E-02
5	+7.6200E+00	+4.4600E+02	+4.6143E+02	-3.4593E+00	+1.0714E-01
6	+9.1440E+00	+3.1400E+02	+3.1303E+02	+3.1049E-01	+2.1615E-01
7	+1.2192E+01	+1.3750E+02	+1.3599E+02	+1.0949E+00	+1.1272E+00
8	+1.5240E+01	+5.7600E+01	+5.7798E+01	-3.4421E-01	+6.4236E+00

CORRELATION MATRIX:

	1	2	3	5	6	7	8	9
1	+1.00	-.89	+.96	+.60	-1.00	+.89	+.37	-.48
2	-.89	+1.00	+.73	+.87	-.92	+1.00	+.71	-.79
3	+.96	+.73	+1.00	-.35	+.94	-.73	-.08	+.20
5	+.60	+.87	-.35	+1.00	+.65	-.87	-.96	+.99
6	-1.00	-.92	+.94	+.65	+1.00	+.91	+.41	-.52
7	+.89	+1.00	-.73	-.87	+.91	+1.00	-.71	+.79
8	+.37	+.71	-.08	-.96	+.41	-.71	+1.00	+.99
9	-.48	-.79	+.20	+.99	-.52	+.79	+.99	+1.00

REDUCED CHI-SQUARED=-31.44
 PHI=31.442

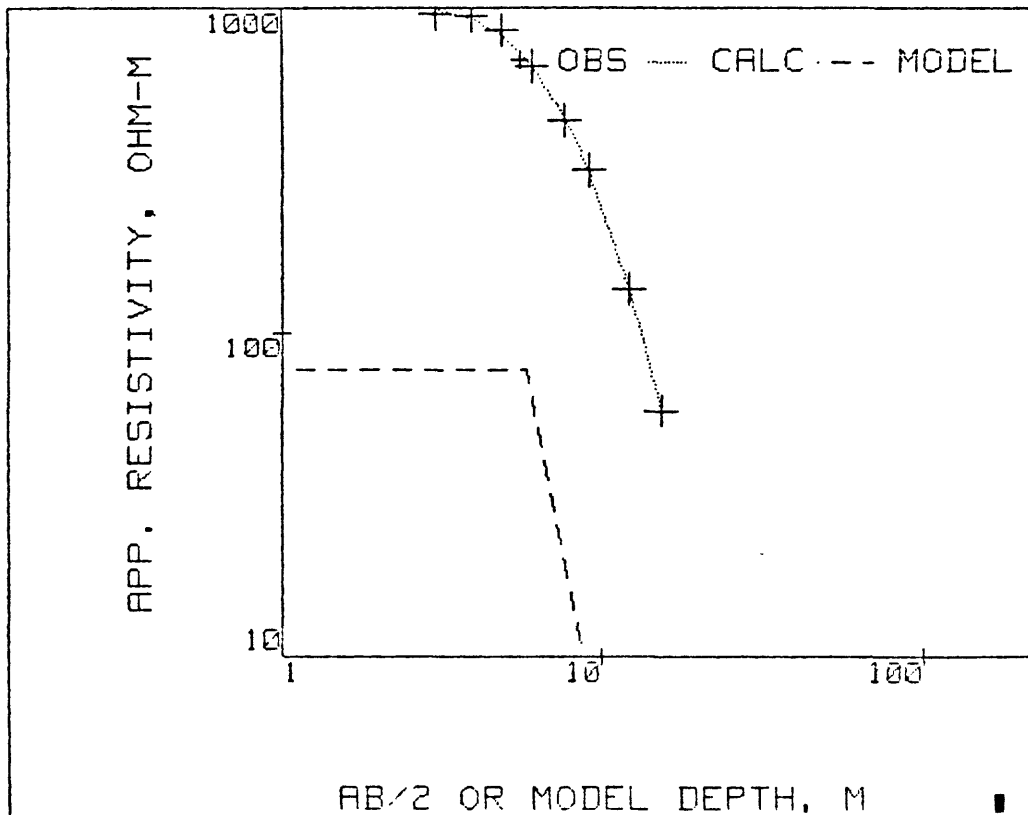
DCLAG: ***** END *****
 COORDINATES: 0 0
 ELEVATION : 0
 AZIMUTH :

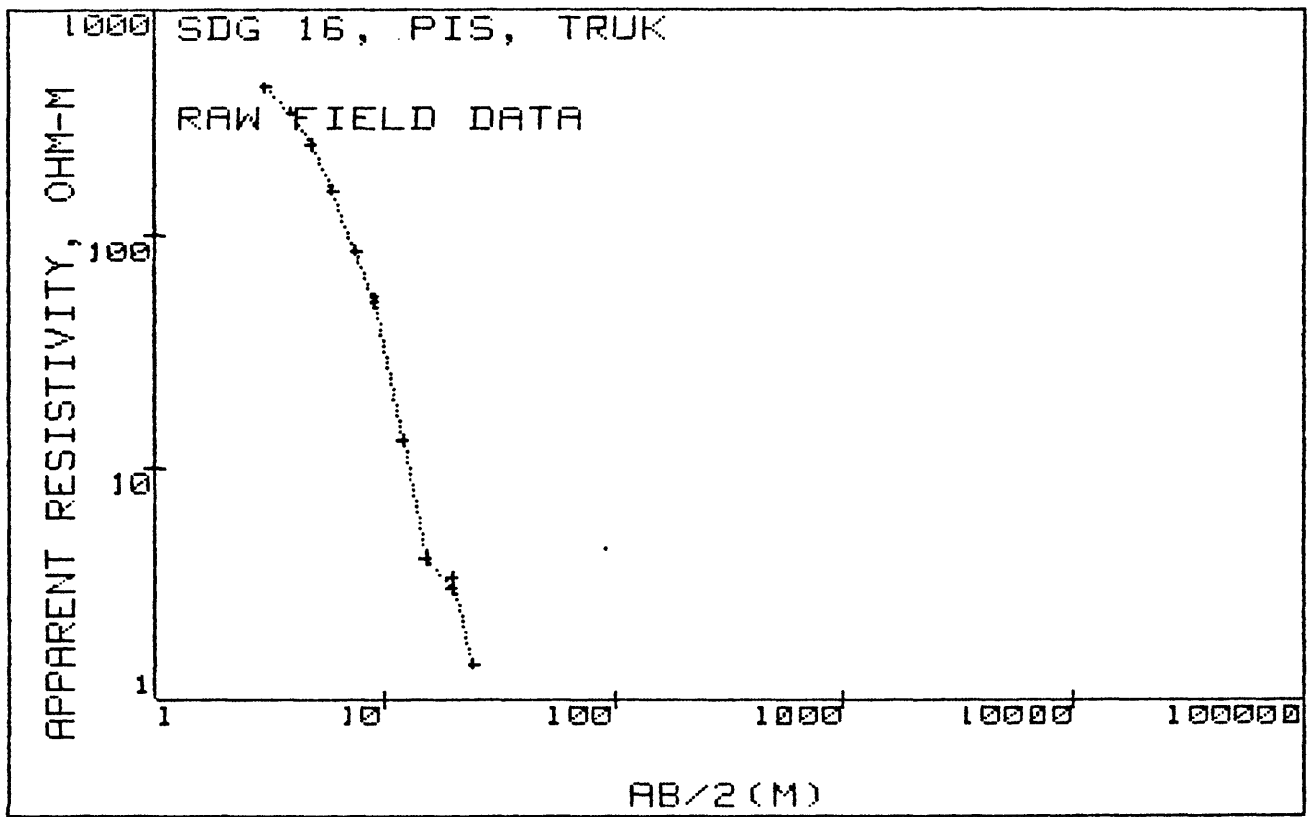
SDG 15, PIS, TRUK

RESISTIVITY		THICKNESS		DEPTH	ELEV
0.0	73.2	0.0	.1	0.0	0.0
0.0	3731.1	0.0	.9	.1	-.1
0.0	76.7	0.0	4.9	1.0	-1.0
*****	-2.0*****	0.0	2.8	5.8	-5.8
0.0	0.0			8.7	-8.7

MODEL HAS LAYERS WHOSE RESISTIVITIES ARE TRANSITIONAL BETWEEN ADJACENT LAYERS:
 RESISTIVITY OF -1 SIGNIFIES LINEAR RESISTIVITY
 RESISTIVITY OF -2 SIGNIFIES LIENAR CONDUCTIVITY

SDG 15, PIS, TRUK





AB/2 (M)	APP. RHO
3.0	455.0
4.0	352.0
4.9	246.0
6.1	157.4
7.6	86.8
9.1	51.0
9.1	53.8
12.2	13.2
15.2	4.1
19.8	3.0
19.8	3.4
24.4	1.4

MARQUARDT STATISTICS: SD6 16, PIS, TRUK

	X	OBSERVED	PREDICTED	%RESIDUALS	WEIGHT FN
1	+3.0480E+00	+5.3898E+02	+5.4393E+02	-8.4442E-01	+6.4342E-05
2	+3.9524E+00	+4.1697E+02	+4.0398E+02	+3.1142E+00	+1.0751E-04
3	+4.8768E+00	+2.9141E+02	+2.9617E+02	-1.6347E+00	+2.2011E-04
4	+6.0960E+00	+1.8645E+02	+1.9075E+02	-2.3039E+00	+5.3766E-04
5	+7.6200E+00	+1.0282E+02	+1.0540E+02	-2.5120E+00	+1.7680E-03
6	+9.1440E+00	+6.0413E+01	+5.6046E+01	+7.2294E+00	+5.1213E-03
7	+1.2192E+01	+1.4823E+01	+1.5109E+01	-1.9303E+00	+8.5074E-02
8	+1.5240E+01	+4.5815E+00	+4.6082E+00	-5.8179E-01	+8.9048E-01
9	+1.9812E+01	+3.3800E+00	+1.7550E+00	+4.8078E+01	+2.6178E-03
10	+2.4384E+01	+1.4400E+00	+1.4366E+00	+2.3693E-01	+9.0140E+00

CORRELATION MATRIX:

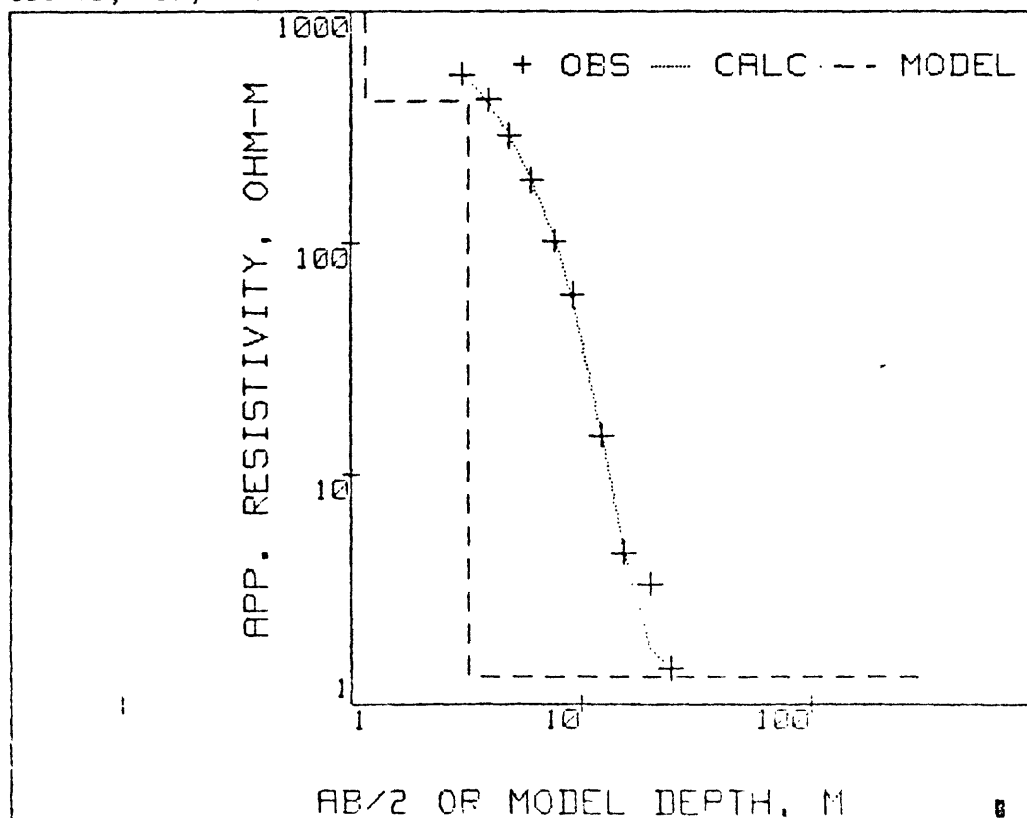
	1	2	3	4	5
1	+1.00	+0.96	+0.08	-0.99	+1.00
2	+0.96	+1.00	+0.14	-0.99	+0.95
3	+0.08	+0.14	+1.00	-0.11	+0.06
4	-0.99	-0.99	-0.11	+1.00	-0.98
5	+1.00	+0.95	+0.06	-0.98	+1.00

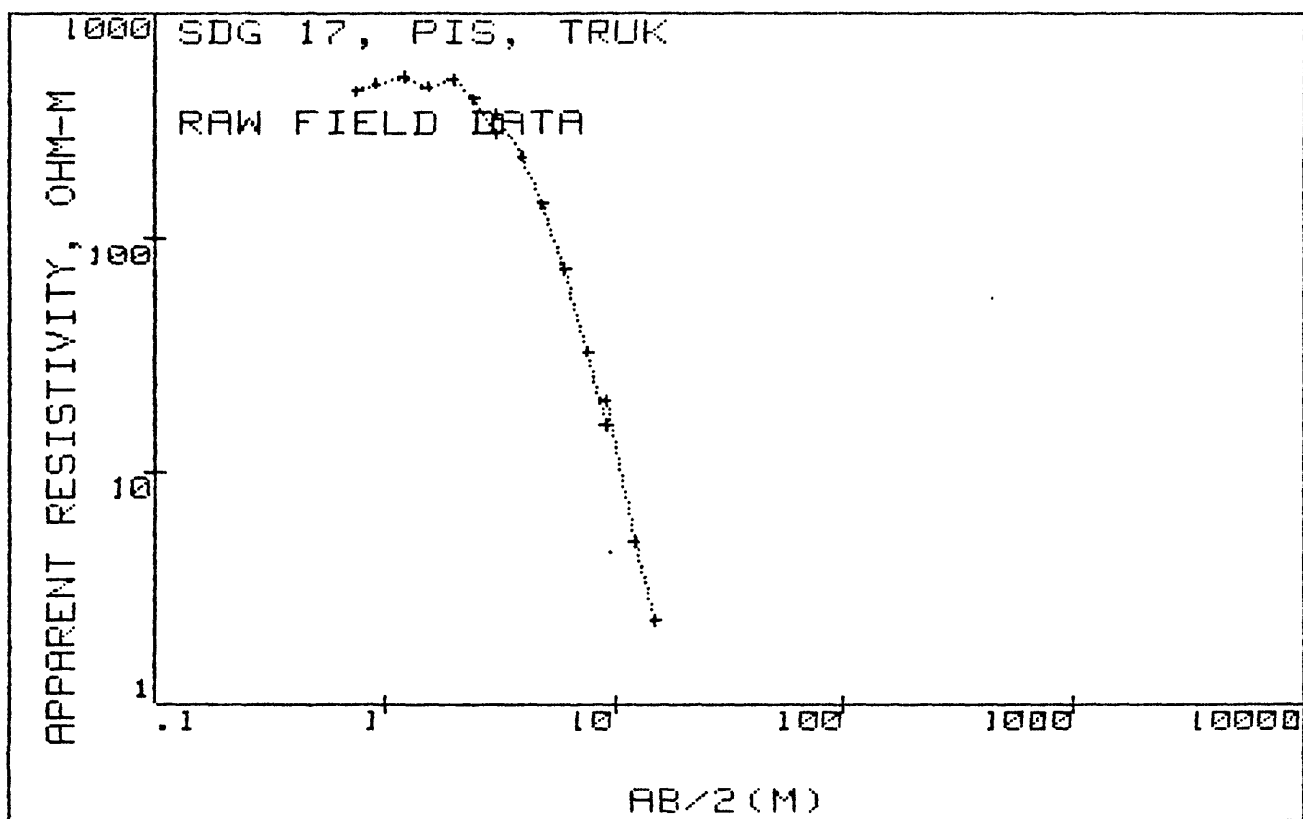
REDUCED CHI-SQUARED=21.2
PHI=84.786

DCLAG: ***** END ***** SD6 16, PIS, TRUK
COORDINATES: 0 0
ELEVATION : 0
AZIMUTH :

RESISTIVITY			THICKNESS			DEPTH	ELEV
0.0	981.2		0.0	1.2		0.0	0.0
0.0	408.6		0.0	2.1	6853.2	1.2	-1.2
.4	1.3	4.1				3.2	-3.2

SD6 16, PIS, TRUK





AB/2 (M) APP. RHO

.8	452.0
.9	489.0
1.2	521.0
1.5	473.0
2.0	508.0
2.4	419.0
3.0	295.0
3.0	358.0
4.0	230.0
4.9	142.4
6.1	75.2
7.6	32.9
9.1	15.7
9.1	20.1
12.2	5.1
15.2	2.3

	X	OBSERVED	PREDICTED	%RESIDUALS	WEIGHT FN
1	+7.6200E-01	+7.0226E+02	+6.9906E+02	+4.5454E-01	+1.2265E-04
2	+9.1440E-01	+7.5974E+02	+7.5498E+02	+6.2674E-01	+1.0479E-04
3	+1.2192E+00	+8.0946E+02	+8.0579E+02	+4.5399E-01	+9.2316E-05
4	+1.5240E+00	+7.3488E+02	+7.9909E+02	-8.6003E+00	+1.1200E-04
5	+1.9912E+00	+7.8926E+02	+7.2391E+02	+8.2807E+00	+9.7101E-05
6	+2.4364E+00	+6.5099E+02	+6.1803E+02	+5.0631E+00	+1.4273E-04
7	+3.0480E+00	+4.5833E+02	+4.7379E+02	-3.3739E+00	+2.8794E-04
8	+3.9624E+00	+2.9446E+02	+2.9916E+02	-1.5970E+00	+6.9762E-04
9	+4.8768E+00	+1.8231E+02	+1.8330E+02	-5.4671E-01	+1.8199E-03
10	+6.0960E+00	+9.6275E+01	+9.4973E+01	+1.3527E+00	+6.5259E-03
11	+7.6200E+00	+4.2120E+01	+4.2535E+01	-9.8378E-01	+3.4094E-02
12	+9.1440E+00	+2.0100E+01	+1.9882E+01	+1.0860E+00	+1.4972E-01
13	+1.2192E+01	+5.0500E+00	+5.0779E+00	-5.5263E-01	+2.3718E+00
14	+1.5240E+01	+2.3000E+00	+2.2961E+00	+1.6830E-01	+1.1434E+01

CORRELATION MATRIX:

	1	2	3	5	6	7	8	9
1	+1.00	+0.88	+0.63	-0.97	+0.90	-0.88	-0.69	+0.72
2	+0.88	+1.00	+0.32	-0.74	+1.00	-1.00	-0.36	+0.40
3	+0.63	+0.32	+1.00	-0.77	+0.33	-0.33	-0.99	+0.99
5	-0.97	-0.74	-0.77	+1.00	-0.76	+0.74	+0.83	-0.85
6	+0.90	+1.00	+0.33	-0.76	+1.00	-1.00	-0.38	+0.42
7	-0.88	-1.00	-0.33	+0.74	-1.00	+1.00	+0.37	-0.41
8	-0.69	-0.36	-0.99	+0.83	-0.38	+0.37	+1.00	-1.00
9	+0.72	+0.40	+0.99	-0.85	+0.42	-0.41	-1.00	+1.00

REDUCED CHI-SQUARED=37.5

PHI=187.52

DLRAG: ***** END *****

SDG 17, PIS, TRUK

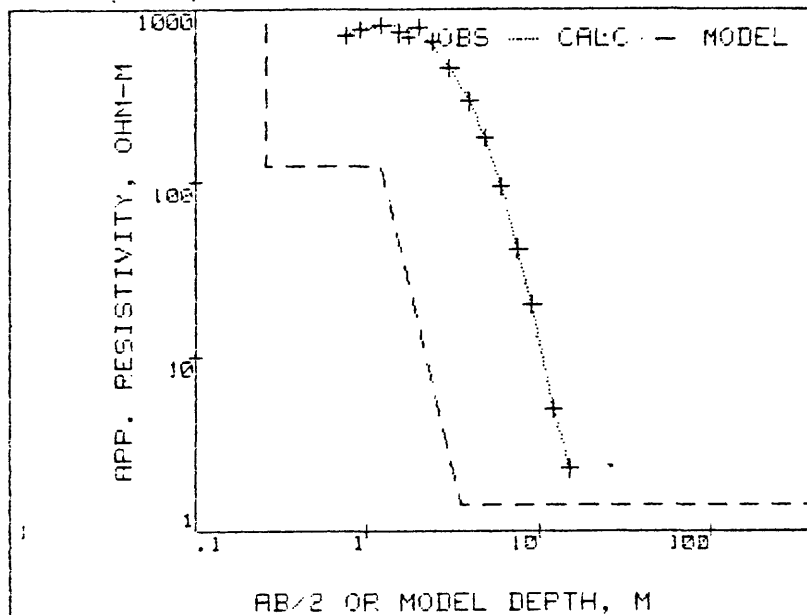
COORDINATES: 0 0

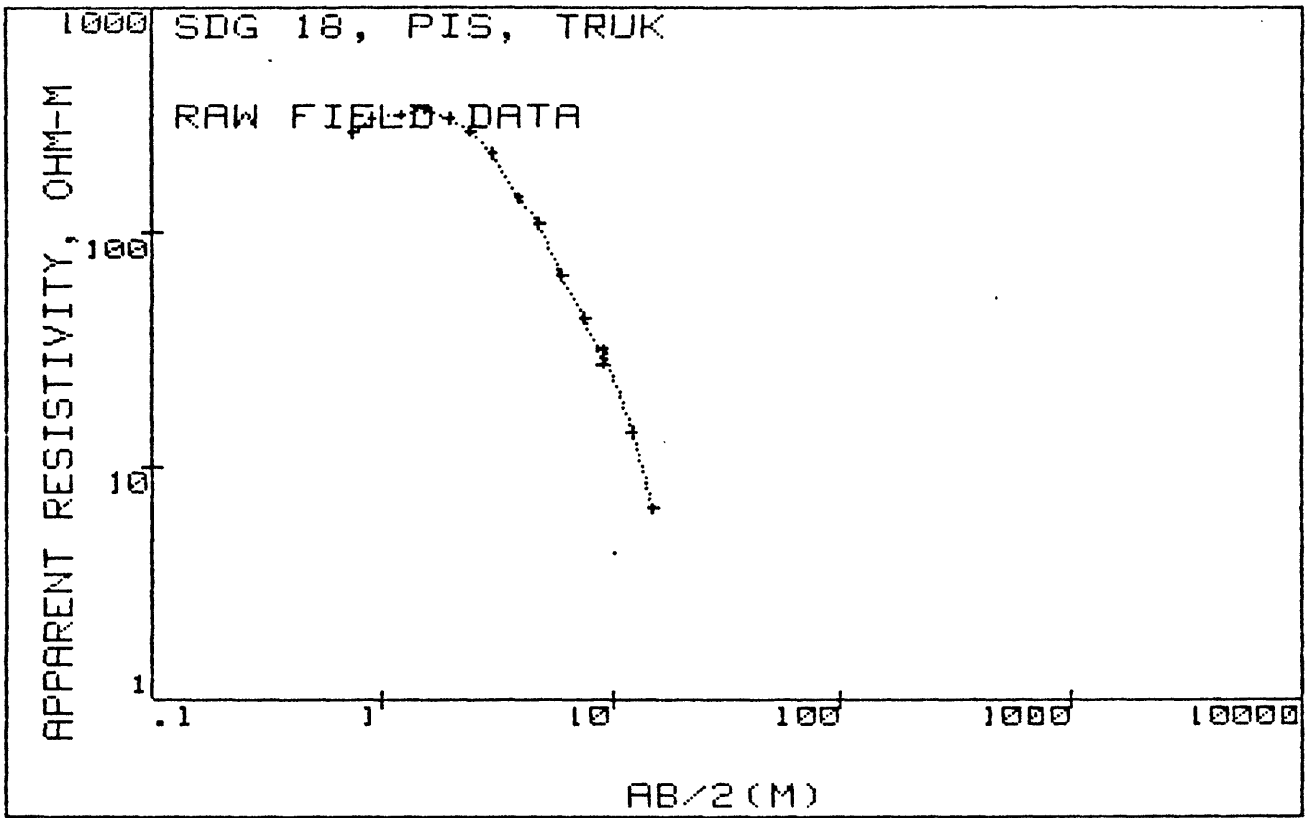
ELEVATION : 0

AZIMUTH :

RESISTIVITY			THICKNESS		DEPTH	ELEV
.1	22.8	8301.5	0.0	0.0	0.0	0.0
0.0	4698.9		0.0	.2	0.0	-0.0
0.0	125.2		0.0	.9	.3	-.3
*****	-1.0*****		0.0	2.3	1.2	-1.2
0.0	1.4				3.5	-3.5

SDG 17, PIS, TRUK





AB/2 (M) APP. RHO

.8	275.0
.9	321.0
1.2	335.0
1.5	355.0
2.0	321.0
2.4	279.0
3.0	224.0
3.0	220.0
4.0	142.4
4.9	109.5
6.1	65.7
7.6	42.6
9.1	27.2
9.1	31.5
12.2	13.9
15.2	6.6

MAFGUARDT STATISTICS: SD6 18, PIS, TRUK

	X	OBSERVED	PREDICTED	%RESIDUALS	WEIGHT FN
1	+7.6200E-01	+3.1279E+02	+3.2812E+02	-4.9019E+00	+4.7880E-03
2	+9.1440E-01	+3.6511E+02	+3.5640E+02	+2.3843E+00	+3.5141E-03
3	+1.2192E+00	+3.8103E+02	+3.8513E+02	-1.0752E+00	+3.2265E-03
4	+1.5240E+00	+4.0378E+02	+3.8675E+02	+4.2175E+00	+2.8732E-03
5	+1.9912E+00	+3.6511E+02	+3.5920E+02	+1.6184E+00	+3.5141E-03
6	+2.4384E+00	+3.1734E+02	+3.1528E+02	+6.4952E-01	+4.6517E-03
7	+3.0480E+00	+2.5478E+02	+2.5291E+02	+7.3230E-01	+7.2165E-03
8	+3.9624E+00	+1.6491E+02	+1.7492E+02	-6.0688E+00	+1.7225E-02
9	+4.8768E+00	+1.2681E+02	+1.2134E+02	+4.3174E+00	+2.9130E-02
10	+6.0960E+00	+7.6086E+01	+7.7905E+01	-2.3904E+00	+8.0917E-02
11	+7.6200E+00	+4.9335E+01	+4.8272E+01	+2.1532E+00	+1.9246E-01
12	+9.1440E+00	+3.1500E+01	+3.1439E+01	+1.9483E-01	+4.7210E-01
13	+1.2192E+01	+1.3900E+01	+1.4026E+01	-9.0419E-01	+2.4245E+00
14	+1.5240E+01	+6.6000E+00	+6.5825E+00	+2.6580E-01	+1.0754E+01

CORRELATION MATRIX:

	1	2	3	4	5	6	7
1	+1.00	-.78	-.97	-.03	+1.00	+.78	-.61
2	-.78	+1.00	+.88	-.51	-.72	-1.00	+.97
3	-.97	+.88	+1.00	-.07	-.95	-.88	+.73
4	-.03	-.51	-.07	+1.00	-.11	+.51	-.71
5	+1.00	-.72	-.95	-.11	+1.00	+.72	-.54
6	+.78	-1.00	-.88	+.51	+.72	+1.00	-.97
7	-.61	+.97	+.73	-.71	-.54	-.97	+1.00

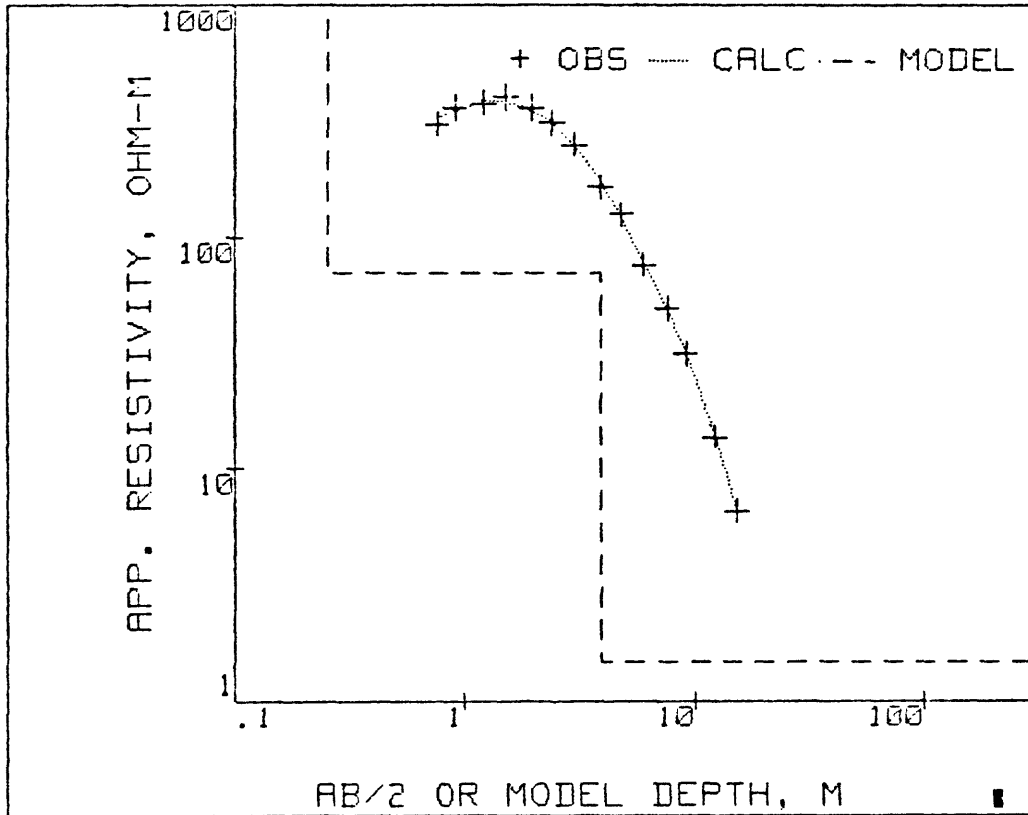
REDUCED CHI-SQUARED=19.83
 PHI=118.98

DCLAG: ***** END *****
 COORDINATES: 0 0
 ELEVATION : 0
 AZIMUTH :

SDG 18, PIS, TRUK

RESISTIVITY			THICKNESS		DEPTH	ELEV
0.0	.8		0.0	0.0	0.0	0.0
0.0	2188.2		0.0	.3	0.0	-0.0
.3	69.4	18956.2	.1	3.7	188.2	-.3
0.0	1.5	1467.5			3.9	-3.9

SDG 18, PIS, TRUK



REFERENCES

- Anderson, W.A., 1979a, Program MARQDCLAG -- Marquardt inversion of Dc-Schlumberger soundings by lagged-convolution: U.S. Geological Survey Open-File Report 79-1432, 58 p.
- Anderson, W.A., 1979b, Program MARQLOOPS -- Marquardt inversion of loop-loop frequency soundings: U.S. Geological Survey Open-File Report 79-240, 75 p.
- Parasnis, D.S., 1979, Principles of Applied Geophysics : John Wiley & Sons, New York, 275 p.
- Raiche, A.P., Jupp, D.L.B., Rutter, H., and Vozoff, K., 1985, The joint use of coincident loop transient electromagnetic and Schlumberger sounding to resolve layered structures : *Geophysics*, v. 50, p. 1618-1627.
- Stark, J.T. and Hay, R.L., 1963, *Geology and Petrology of volcanic rocks of the Truk Islands, Eastern Caroline Islands*: U.S. Geological Survey Professional Paper 409, 41 p.
- Takasaki, K., 1983, Truk Islands -- Hydrologic conditions, April 1-15, 1983, Administrative Report, 9 pp.

LIST OF FIGURES

Figure 1. Map of Truk lagoon showing the high, volcanic islands of Moen, Dublon, Fefan, Uman, Udot, and Tol and the low, coralline island of Pis.

Figure 2. a) Map of Moen, Truk showing the location of a profile of Schlumberger soundings, A-A', and the location of Schlumberger soundings 4, 5, and 6 near Nemwan. b) a pseudo-section showing the resistivities interpreted from Schlumberger soundings 1 through 3. The resistivities are indicated beneath the sounding number.

Figure 3. a) Map of Dublon, Truk showing the location of a profile of Schlumberger soundings B-B', and the location of Schlumberger sounding 11 near the towns of Nechap and Chun. b) a geoelectric cross-section derived from the interpretations of Schlumberger soundings 7 through 10 near Roro. The resistivities are indicated beneath the soundings number. Hydrogeologic interpretations of geoelectric units are labeled.

Figure 4. Map of Fefan, Truk showing the location of Schlumberger soundings 12 and 13.

Figure 5. Map of Pis Island, Truk showing the location of two profiles along which five-frequency Max/Min measurements and Schlumberger soundings 14 through 18 were made.

Figure 6. a) Geoelectric cross-section compiled from interpretations of Max/Min stations 1-1 through 1-6, Schlumberger soundings 14 through 16, and the chloride content of nearby dug wells. The resistivity of the basal conductor (presumed to be seawater-saturated coralline material) is plotted midway between the Max/Min loop stations (pluses). Boxes beneath Schlumberger sounding numbers indicate thickness of the model transition zone. b) same as Figure 6a except compiled from interpretations of Max/Min stations 2-1 through 2-4 and Schlumberger soundings 17 and 18. Ground surface is shown as a horizontal dashed line.

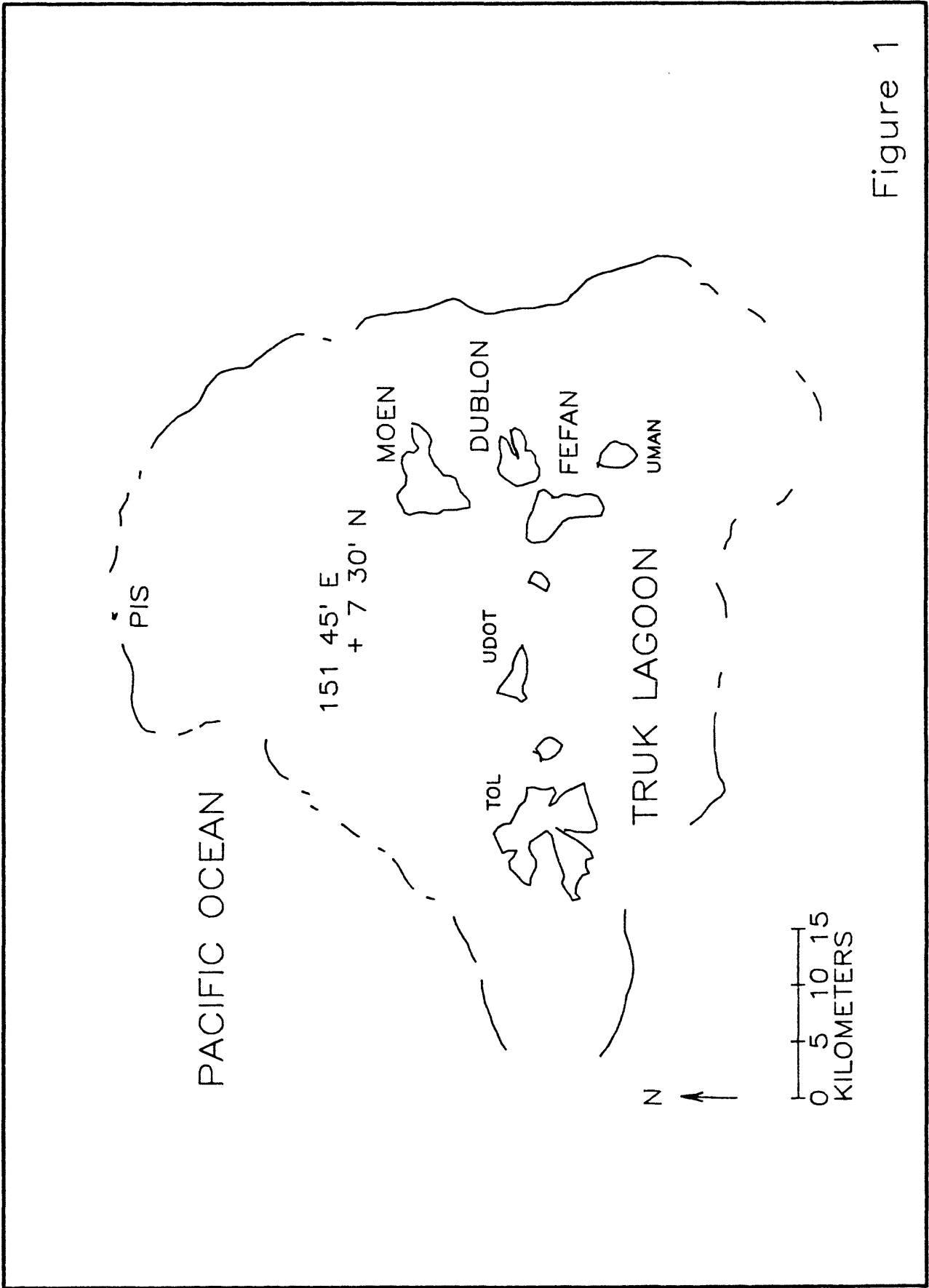


Figure 1

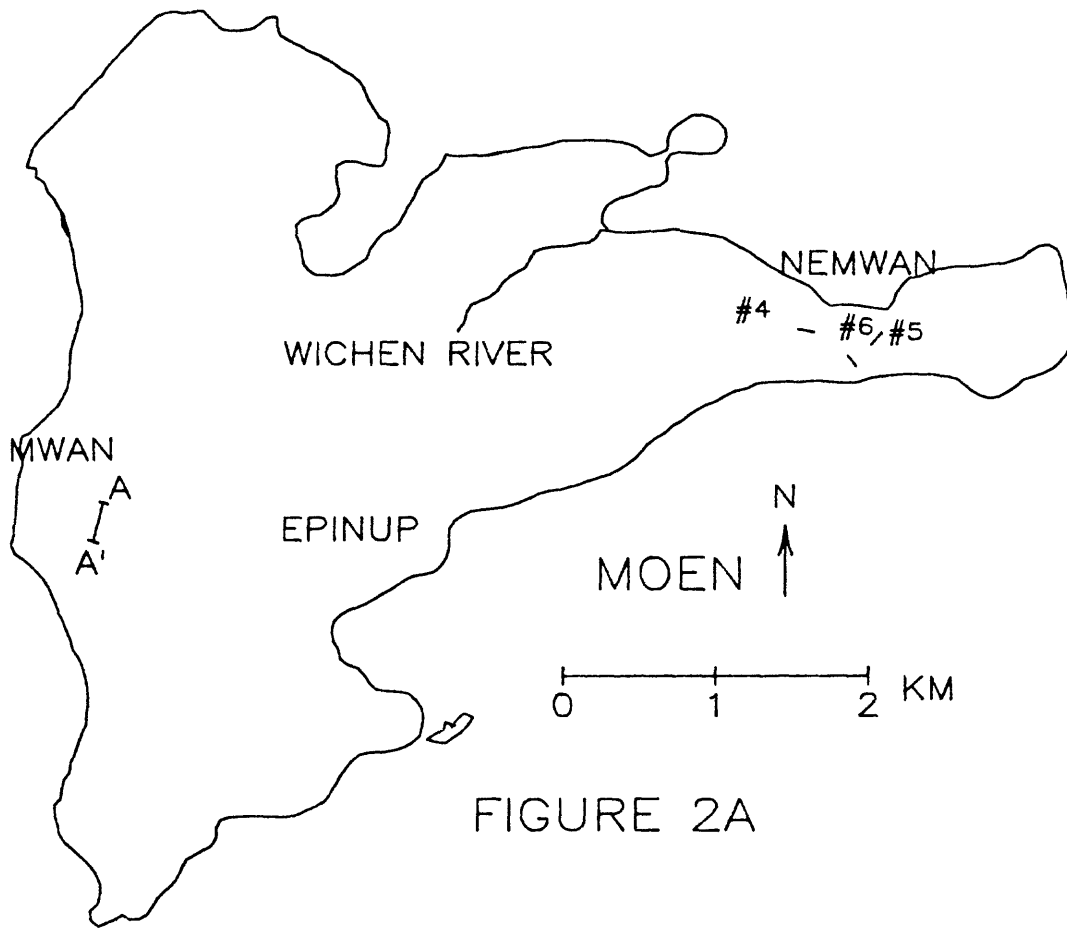


FIGURE 2A

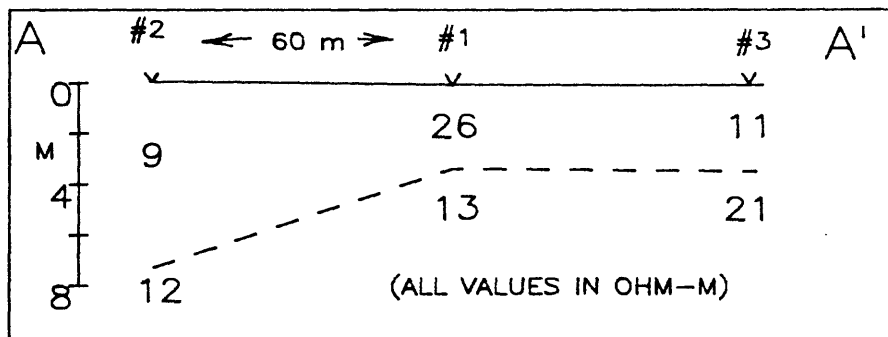


FIGURE 2B

FIGURE 3A DUBLON

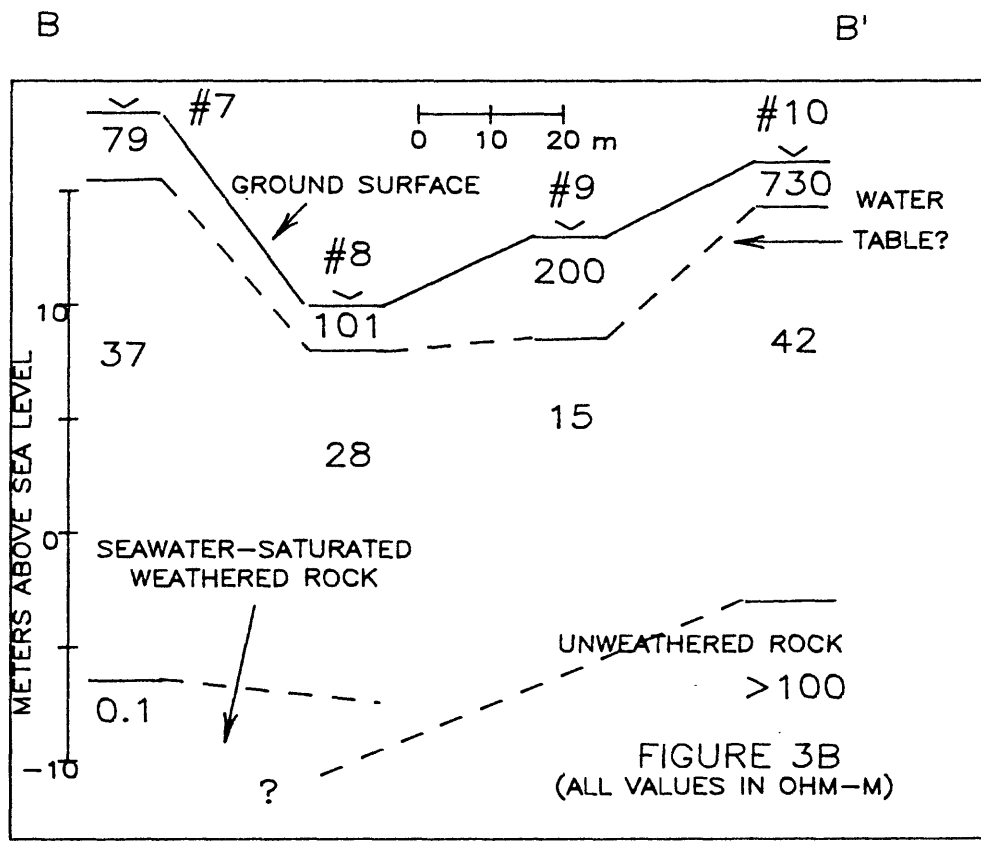
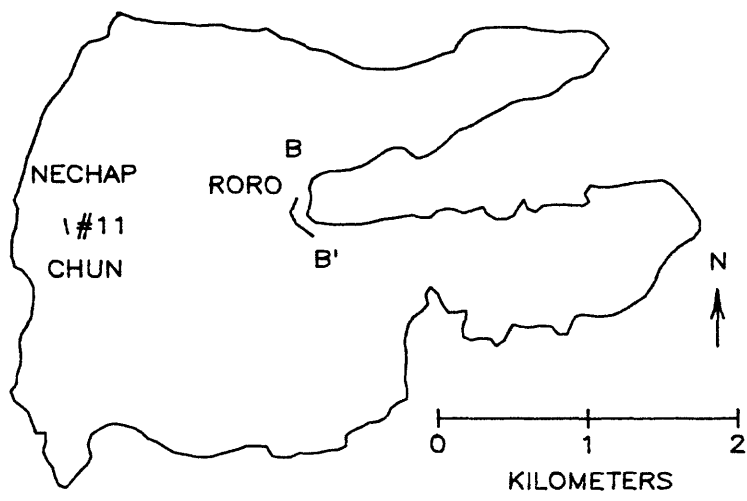


FIGURE 3B
(ALL VALUES IN OHM-M)

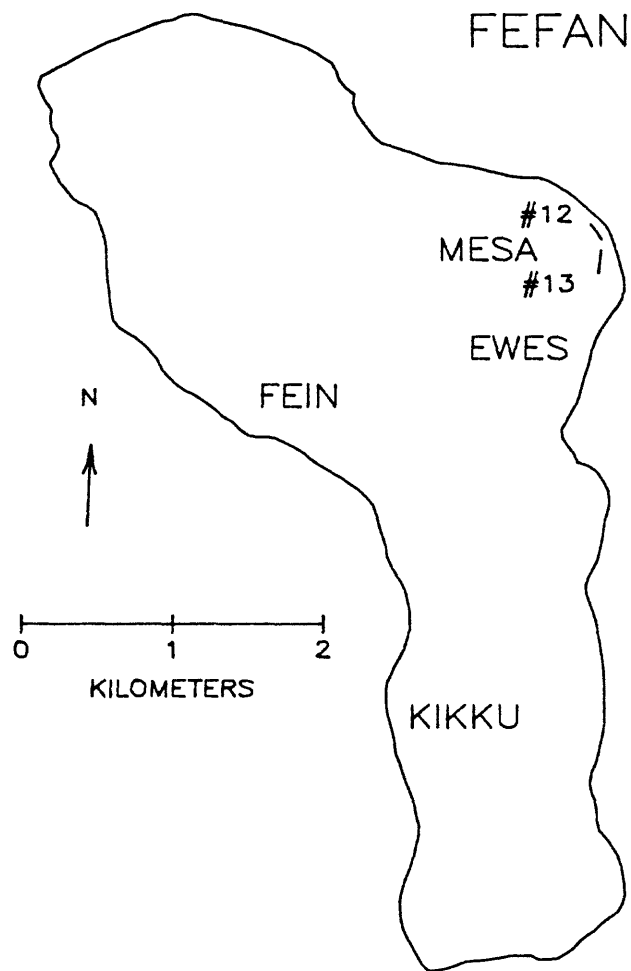


Figure 4

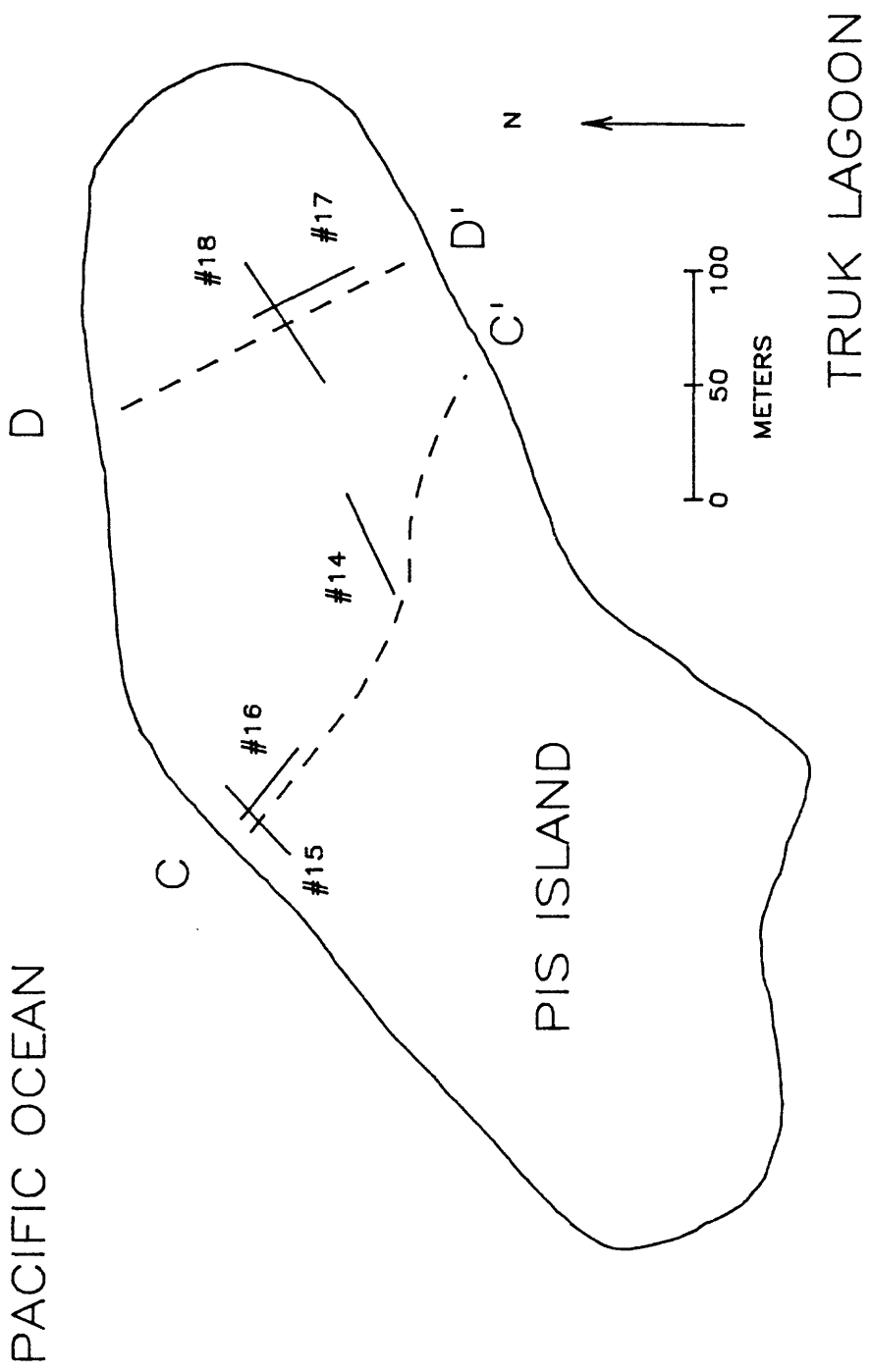


Figure 5

